Acute inflammation sensitizes knee-innervating sensory neurons and decreases mouse digging behavior in a TRPV1-dependent manner.

Sampurna Chakrabarti, Luke A. Pattison, Kaajal Singhal, James R.F. Hockley, Gerard Callejo, and Ewan St. John Smith

Department of Pharmacology, University of Cambridge, Cambridge, UK

Corresponding author: Ewan St. John Smith

Department of Pharmacology, University of Cambridge

Tennis Court Road, Cambridge CB2 1PD

Phone: +44 1223 334048, Fax: +44 1223 334100 Email: es336@cam.ac.uk, Lab URL: https://www.phar.cam.ac.uk/research/Smith

Number of text pages (w tables and figs): 46

Number of figures: 6

Number of tables: 2

Number of Supplementary materials: 2

Abstract

Ongoing, spontaneous pain is characteristic of inflammatory joint pain and reduces an individual's quality of life. To understand the neural basis of inflammatory joint pain, we made a unilateral knee injection of complete Freund's adjuvant (CFA) in mice, which reduced their natural digging behavior. We hypothesized that sensitization of knee-innervating dorsal root ganglion (DRG) neurons underlies this altered behavior. To test this hypothesis, we performed electrophysiological recordings on retrograde labelled knee-innervating primary DRG neuron cultures and measured their responses to a number of electrical and chemical stimuli. We found that 24-hours after CFA-induced knee inflammation, knee neurons show a decreased action potential generation threshold, as well as increased GABA and capsaicin sensitivity, but have unaltered acid sensitivity. The inflammation-induced sensitization of knee neurons persisted for 24-hours in culture, but was not observed after 48-hours in culture. Through immunohistochemistry, we showed that the increased knee neuron capsaicin sensitivity correlated with enhanced expression of the capsaicin receptor, transient receptor potential vanilloid 1 (TRPV1) in knee-innervating neurons of the CFA-injected side. We also observed an increase in the co-expression of TRPV1 with tropomyosin receptor kinase A (TrkA), which is the receptor for nerve growth factor (NGF), suggesting that NGF partially induces the increased TRPV1 expression. Lastly, we found that systemic administration of the TRPV1 antagonist A-425619 reversed the decrease in digging behavior induced by CFA injection, further confirming the role of TRPV1, expressed by knee neurons, in acute inflammatory joint pain.

Keywords: joint pain, inflammation, TRPV1, dorsal root ganglion neurons, digging behavior

1. Introduction

Pain is protective, but its dysregulation has a negative impact on an individual's life, as well as a wider socioeconomic impact (St. John Smith, 2018; Vilen et al., 2017). Inflammatory joint pain is characteristic of many musculoskeletal disorders, often being more diffuse and longer lasting than cutaneous pain (Lewis, 1938). Numerous animal models of inflammatory joint pain are used experimentally (Gregory et al., 2013) and intra-articular complete Freund's adjuvant (CFA) was chosen for use in this study because it produces robust, unilateral inflammation, alongside behavioral hyperalgesia (Keeble et al., 2005). Although spontaneous pain is a hallmark of joint pain, most rodent studies focus on evoked pain behaviors (Arendt-Nielsen, 2017; Schaible et al., 2002). Therefore, shifting the emphasis to study natural behaviors during painful conditions and their underlying molecular mechanisms might facilitate the translation of novel analgesics into clinics (Arendt-Nielsen, 2017).

A variety of techniques have been employed to better understand the molecular drivers of pain. For example, single cell RNA-sequencing studies have characterized dorsal root ganglia (DRG) neurons into distinct subpopulations (Hockley et al., 2018; Li et al., 2015; Usoskin et al., 2015), and electrophysiology and immunohistochemistry have shown that joint innervating DRG neurons possess distinct neurochemical and electrophysiological properties (da Silva Serra et al., 2016). These reports highlight the importance of specifically studying knee neurons, to fully understand the neural basis of joint pain.

Multiple ion channels are involved in transducing noxious stimuli; of these, the Transient Receptor Potential (TRP) channel family are critical to nociceptor chemosensitivity (Moore et al.,

44 2018). Alongside endogenous mediators released during inflammation, e.g. protons, we have
45 shown that articular neurons can be activated by the TRP channel agonists capsaicin (TRPV1),
46 cinnamaldehyde (TRPA1) and menthol (TRPM8) (da Silva Serra et al., 2016). In relation to this,
47 TRPV1$^{-/-}$ and TRPA1$^{-/-}$ mice show reduced pain behavior in CFA models of articular nociception
48 (Chen et al., 2009; Fernandes et al., 2016). Although not tested after CFA-induced joint
49 inflammation, TRPM8$^{-/-}$ mice develop similar mechanical hyperalgesia to wildtype mice following
50 CFA injection into the footpad (Caceres et al., 2017). Joint acidosis correlates with increased
51 severity of inflammatory arthritis in humans, and acidic solutions activate and sensitize rodent
52 nociceptors (Farr et al., 1985; Smith et al., 2011). Mice lacking the proton-gated ion channels acid-
53 sensing ion channel 3 (ASIC3) and TRPV1 have reduced mechanical hyperalgesia following intra-
54 articular CFA injection (Hsieh et al., 2017), but not following subcutaneous hind paw CFA
55 injection, suggesting regional differences in pain processing (Staniland and McMahon, 2009).
56 Subsequently, using magnetic resonance spectroscopic imaging, we found no evidence of tissue
57 acidosis following subcutaneous CFA injection (Wright et al., 2018), suggesting absence of a key
58 stimulus for ASIC3/TRPV1 activation, hence perhaps explaining the lack of phenotype observed
59 in the hind paw CFA model. However, it remains unknown how proton-gated channels contribute
60 to knee-innervating neuron activation during acute inflammation.

61 Regardless of the stimulus, once activated, sensory neuron input to the spinal cord is pre-
62 synaptically modulated by $GABA_A$ receptor signaling, the source of GABA being spinal cord
63 interneurons (Sutherland et al., 2002). In adults, due to the high intracellular [Cl^-] in DRG neurons
64 compared to central nervous system neurons, activation of $GABA_A$ receptors produces
65 depolarization through Cl^- efflux (Chen et al., 2014). Furthermore, after subcutaneous CFA-
66 induced inflammation in rat paws, the magnitude of GABA-evoked currents is increased in

67 cutaneous DRG neurons (Zhu et al., 2012), as well as in isolated human DRG neurons incubated
68 in an inflammatory soup (Zhang et al., 2015). However, the characteristics of GABA-evoked
69 currents in knee-innervating neurons, and their modulation during inflammation are unknown.

70 Here, we hypothesized that sensitization of knee-innervating neurons following CFA-
71 induced knee inflammation underlies changes in natural behavior.

72 2. Methods

73 *2.1.Animals*

74 All mice used in this study were 6-15 week old female C57BL/6J (Envigo); female mice
75 were used because being female is a risk factor for inflammatory pain (Hannan, 1996). We did not
76 control for estrus cycle because C57BL/6 mice show relatively stable behavior across the four
77 stages of estrus, including pain behaviors (Meziane et al., 2007). Mice were conventionally housed
78 in groups of 4-5 with nesting material and a red plastic shelter; the holding room was temperature
79 controlled (21 °C) and mice were on a normal 12 hour/light dark cycle with food and water
80 available *ad libitum.* This research was regulated under the Animals (Scientific Procedures) Act
81 1986 Amendment Regulations 2012 following ethical review by the University of Cambridge
82 Animal Welfare and Ethical Review Body.

83

84 *2.2.Knee joint intra-articular injections*

85 Under anesthesia (ketamine, 100 mg/kg and xylazine, 10 mg/kg, i.p.) a single injection of
86 the retrograde tracer Fast Blue (FB; 1.5 µl 2% in 0.9 % saline; Polysciences) was made intra-
87 articularly through the patellar tendon into each knee to label knee-innervating neurons. For all
88 experiments, anaesthetized mice were injected with 7.5 µl Complete Freund's adjuvant (CFA; 10

89 mg/ml; Chondrex) intra-articularly through the patellar tendon in the left knee seven days after
90 administration of FB. Knee width was measured with Vernier's calipers before and 24-hours after
91 CFA injection.

92

93 *2.3.Digging behavior paradigm*

94 Digging behavior testing was carried out in a subset of mice used for electrophysiological
95 and immunohistochemistry studies. A standard 49 x 10 x 12 cm cage with a wire lid, filled with
96 Aspen midi 8/20 wood chip bedding (LBS Biotechnology) tamped down to a depth of ~ 4 cm, was
97 used as the test environment. Each mouse was tested individually using fresh bedding. Testing
98 lasted three minutes and to avoid distractions food and water were not available. All digging
99 experiments were carried out between 12:00 and 14:00 on weekdays in the presence of one male
100 and one female experimenter.

101 **2.3.1. Testing protocol for assessing the impact of CFA-induced inflammation:**

102 Each day before assessment of digging, mice were habituated in the procedure room, in
103 their home cage, for 30 min. On the training days (2 days before FB or CFA injection in the knee,
104 Figure 1A) mice were allowed to dig twice, with a 30-minute break between sessions. All
105 subsequent days were test days and, after habituation, mice were allowed to dig once. Test digs
106 were recorded and the digging duration (time mice spent actively displacing bedding material with
107 their front and hind limbs), as well as the number of visible burrows (crater-like sites in the cage
108 with displaced bedding material) in test cages were counted immediately after the 3-minute test
109 session. Digging duration was scored independently by the two experimenters by watching video

110 recordings. Since the scores were well correlated (Pearson correlation $R^2 = 0.93$), an average is
111 reported.

112 **2.3.2. Testing protocol for assessing the effect of TRPV1-antagonist, A-425619:**

113 Seventeen mice were trained as above and the day before CFA knee injections their digging
114 behavior was measured twice with a 30 min interval in between. Since the digging duration (saline
115 group: Run 1, 30.3 ± 7.1 s vs. Run 2, 33.8 ± 6.4 s, $t(6) = 0.39$, $p = 0.7$, $n = 7$; CFA group: Run 1,
116 32.2 ± 5.1 s vs. Run 2, 31.1 ± 6.1 s, $t(9) = 0.21$, $p = 0.8$, $n = 10$, paired t-test) and number of
117 burrows (saline group: Run 1, 3.4 ± 0.4 vs. Run 2, 3.4 ± 0.4, $t(6) = 0.0$, $p > 0.9$, $n = 7$; CFA group,
118 Run 1, 4.0 ± 0.3 vs. Run 2, 4.3 ± 0.4, $t(9) = 1.1$, $p = 0.3$, $n = 10$, paired t-test) did not change
119 between these two test digs for either group, the measurement from the second run is reported as
120 pre-CFA/saline. On the day of the injection, the mice were randomly split into two groups: the
121 CFA group received CFA in one knee (as described above) and the control group received saline
122 in one knee. 24-hours after the injections, digging activity was re-assessed, after which all mice
123 received an intra-peritoneal dose of the TRPV1 antagonist, A-425619 (100 μmol/kg, Tocris, made
124 up in 10% DMSO and 34% 2-hydroxylpropyl β-cyclodextrin, Sigma-Aldrich, in dH_2O). Digging
125 activity was measured again after 30 min as previous reports show maximal anti-nociceptive effect
126 of A-425619 at this time point (Hillery et al., 2011). At the end of the study all the videos of test
127 digs were independently assessed by the experimenters, who were blinded to the treatment
128 conditions and stage of the experiment by an assistant, and an average of their scores is reported.

129

130 *2.4.DRG neuron culture*

131 Following cervical dislocation and decapitation, the spinal column was dissected and the
132 lumbar (L2 to L5) DRG (that primarily innervate the knee joint) were collected (da Silva Serra et
133 al., 2016; Rigaud et al., 2008). DRG from the CFA-injected and non-injected sides were separately
134 collected in ice cold dissociation media containing L-15 Medium (1X) + GlutaMAX-l (Life
135 Technologies), supplemented with 24 mM $NaHCO_3$. DRG were then incubated in 3 ml type 1A
136 collagenase (1 mg/ml with 6 mg/ml bovine serum albumin (BSA) in dissociation media; Sigma-
137 Aldrich) for 15 min at 37 °C, followed by 30 min incubation in 3 ml trypsin solution (1 mg/ml
138 with 6 mg/ml BSA in dissociation media; Sigma-Aldrich) at 37 °C. After removing the enzymes,
139 the DRG were suspended in culture media containing L-15 Medium (1X) + GlutaMAX-l, 10 %
140 (v/v) fetal bovine serum, 24 mM $NaHCO_3$, 38 mM glucose, 2 % penicillin/streptomycin,
141 dissociated by mechanical trituration with a 1 ml Gilson pipette and briefly centrifuged (160 g, 30
142 s; Biofuge primo, Heraeus Instruments; Hanau, Germany). Supernatants containing dissociated
143 DRG neurons were then collected in a fresh tube. This was repeated five times. Finally, the cells
144 were plated onto poly-D-lysine and laminin coated glass bottomed dishes (MatTek, P35GC-1.5-
145 14-C) and incubated (37 °C, 5 % CO_2) for 4-, 24- or 48-hours depending upon the experiment.

146

147 *2.5.Immunohistochemistry*

148 FB labelled and CFA-injected mice were transcardially perfused, firstly with PBS,
149 followed by 4 % (w/v) paraformaldehyde (PFA; in PBS, pH 7.4) under terminal anesthesia
150 (sodium pentobarbital; 200 mg/kg, i.p.). L2 – L5 DRG were collected from the CFA-injected and
151 non-injected sides and post-fixed for 1-hour (4 % PFA), followed by an overnight incubation in
152 30 % (w/v) sucrose (in PBS) at 4 °C for cryoprotection. DRG were next embedded in Shandon M-
153 1 Embedding Matrix (Thermo Fisher Scientific), snap frozen in 2-methylbutane (Honeywell

154 International) on dry ice and stored at -80 °C. Embedded DRG were sectioned (12 μm) using a
155 Leica Cryostat (CM3000; Nussloch, Germany), mounted on Superfrost Plus microscope slides
156 (Thermo Fisher Scientific) and stored at -20 °C until staining. One to three sections were chosen
157 at random for analysis from each CFA-injected and contralateral side of four mice.

158 Slides were defrosted, washed with PBS-tween and blocked in antibody diluent solution:
159 0.2 % (v/v) Triton X-100, 5 % (v/v) donkey serum and 1 % (v/v) bovine serum albumin in PBS
160 for 1-hour at room temperature before overnight incubation at 4 °C with primary antibodies anti-
161 TRPV1 (1:1000, rabbit polyclonal, Abcam ab31895) and anti-TrkA (1:1000, goat polyclonal,
162 R&D systems AF1056) in antibody diluent. Slides were washed three times using PBS-tween and
163 incubated with species-specific conjugated secondary antibodies (1:1000, anti-rabbit Alexa-488
164 (Invitrogen, A21206) and anti-goat Alexa-568 (Invitrogen, A11057)) for 2-hours at room
165 temperature (20-22 °C). Slides were washed in PBS-tween, mounted and imaged with an Olympus
166 BX51 microscope (Tokyo, Japan) and QImaging camera (Surrey, Canada). Exposure levels were
167 kept constant for each slide and the same contrast enhancements were made to all slides. Negative
168 controls without the primary antibody showed no staining with either secondary.

169 Using ImageJ, the mean gray value of each neuron in a DRG section was measured and
170 normalized between the highest and lowest intensity neuron for that section. The threshold used
171 for scoring a neuron as positive for a stain was set as the normalized minimum gray value across
172 all sections + 2 times SD.

173

174 *2.6. Whole cell patch-clamp electrophysiology*

175 At least three DRG neurons from the CFA-injected side (CFA) and contralateral (Cntrl)
176 side from each animal were recorded. To try and maintain an even distribution of animals across
177 all time points at which recordings were made, the same culture was used for 4-hours, 24-hours
178 and 48-hours wherever possible, however, due to the paucity of labelled neurons and variability of
179 culture conditions, this was not possible in some cases. In total, each of the conditions contained
180 DRG neurons from 6-8 mice. At each time point recordings were made for-4 hours. The
181 extracellular solution contained (in mM): NaCl (140), KCl (4), $MgCl_2$ (1), $CaCl_2$ (2), glucose (4)
182 and HEPES (10) adjusted to the required pH (> 6.0) with NaOH. For solutions with pH < 6.0, MES
183 was used instead of HEPES. Patch pipettes of 4-9 MΩ were pulled with a P-97 Flaming/Brown
184 puller (Sutter Instruments; Novato, CA, USA) from borosilicate glass capillaries and the
185 intracellular solution used contained (in mM): KCl (110), NaCl (10), $MgCl_2$ (1), EGTA (1),
186 HEPES (10), Na_2ATP (2), Na_2GTP (0.5) adjusted to pH 7.3 with KOH. Recordings were made
187 using a HEKA EPC-10 amplifier (Lambrecht, Germany) and the corresponding Patchmaster
188 software. FB labelled neurons were identified by their fluorescence upon excitation with a 365nm
189 LED (Cairn Research; Faversham, United Kingdom). For all experiments, DRG neurons were held
190 at -60 mV and whole cell currents were acquired at 20 kHz. Only neurons where an action potential
191 (AP) could be evoked in response to current injections and had a resting membrane potential more
192 negative than -40 mV were analyzed. Images of neurons were captured using a 40x objective on a
193 Nikon Eclipse Ti-S microscope and a Zyla 5.5 sCMOS camera (Andor; Belfast, United Kingdom),
194 followed by pixel to μm conversion to calculate their diameter using ImageJ software.

195 **2.6.1. Testing Protocols:**

196 **Action potential generation:** APs were generated by 80 ms current injections of 150-1050 pA in
197 50 pA steps (Figure 2A). If an AP was generated at 150 pA, the neuron was retested with current

198 injections of 0–1000 pA, in 50 pA steps. Threshold, amplitude, half peak duration (HPD),
199 afterhyperpolarization (AHP) duration and AHP amplitude (Figure 2A) were measured using
200 Fitmaster software (HEKA) or IgorPro software (Wavemetrics) as described before (Bonin et al.,
201 2013; Djouhri et al., 2001; Kim et al., 1998). AP amplitude is defined as the peak of the AP from
202 the repolarized membrane potential; HPD is the AP width at half-amplitude, AHP was obtained
203 by fitting the decay to a single exponential function and AHP amplitude was obtained by
204 subtracting the peak voltage during AHP from the repolarized membrane potential (see Figure 2A
205 for more detail).

206 **Acid sensitivity and TRP-agonist sensitivity:** Solutions for determining acid sensitivity (pH 7,
207 pH 6, pH 5) and TRP-agonist sensitivity (capsaicin, cinnamaldehyde and menthol) were applied
208 in a random order through a gravity-driven 12 barrel perfusion system (Dittert et al., 2006) to DRG
209 neurons in 5 s pulses with at least 30 s wash period (with pH 7.4) between stimuli. Solutions of 10
210 μM capsaicin (1 mM stock in 100% ethanol; Sigma-Aldrich), 100 μM cinnamaldehyde (10 mM
211 stock in 100% ethanol; Merck) and 100 μM menthol (20 mM stock in 100% ethanol; Alfa Aesar)
212 were made up in pH 7.4 extracellular solution from their respective stock solutions. Control
213 experiments (n = 3) with ethanol did not evoke any currents from neurons. Current amplitude was
214 measured in Fitmaster (HEKA) by subtracting the maximum peak response from the baseline
215 (average of the first 3 s before stimulation), which was then normalized by dividing by neuron
216 capacitance to give current density.

217 **GABA sensitivity:** 100 μM GABA (100 mM stock in water; Sigma-Aldrich) was applied for 5 s
218 followed by a 20 s wash with pH 7.4, then 100 μM GABA and 250 μM bicuculline (100 mM in
219 DMSO; Sigma-Aldrich) were applied together for 5 s. Recovery from bicuculline block was
220 assessed after 1 min by a subsequent 100 μM GABA application for 5 s. To test for the presence

221 of the $GABA_A$-δ subunit, 100 μM of the δ agonist 4,5,6,7-tetrahydroisoxazolo[5,4-c]pyridin-3-ol
222 hydrochloride (THIP, 100 mM stock in distilled water; Sigma-Aldrich) was applied for 5 s.
223
224 *2.7.Statistical Analysis*
225 Comparison of CFA and Cntrl neuron electrophysiological properties was performed using
226 a Student's unpaired t-test (two-sided), while comparison across time (4-hours, 24-hours and 48-
227 hours) was made using a one-way ANOVA followed by a Holm-Sidak multiple comparison test.
228 To compare proportions in patch-clamp and immunostaining experiments, a chi-squared test was
229 used. Knee width before and after inflammation with CFA was compared using a Student's paired
230 t-test (two-sided). Digging behavior of mice in different groups was compared using a repeated
231 measures one-way ANOVA followed by a Holm-Sidak multiple comparison test. Data are
232 presented as mean ± standard error of mean.
233
234
235
236
237
238
239
240
241

242 3. Results

243 *3.1.Inflammation and reduced well-being in mice after unilateral knee joint CFA injection*

244 Injection of CFA into the knee joint produces acute and chronic inflammatory pain in mice
245 that models human arthritis (Gauldie et al., 2004). To produce acute inflammation, 7-days after
246 labelling knee-innervating neurons by FB injection, CFA was injected into the left knee joint of
247 mice (timeline in Figure 1A). After 24-hours, we observed robust swelling indicative of edema
248 and inflammation of the ipsilateral knee (pre-CFA, 3.8 ± 0.07 mm vs. post-CFA, 4.6 ± 0.06 mm,
249 $t(16) = 22.2$, $p < 0.0001$, $n = 17$, paired t-test), but not the contralateral knee (pre-CFA, 3.7 ± 0.07
250 mm vs. post-CFA, 3.7 ± 0.06 mm, $n =17$, $t(16) = 0.0$, $p > 0.9$, paired t-test, Figure 1B, 1C); a pilot
251 study found that FB injection alone induced no change in knee width ($n = 6$, pre-FB, 3.9 ± 0.05
252 mm, post-FB, 4.0 ± 0.05 mm, $t(5) = 0.89$, $p = 0.4$, paired t-test)

253 Spontaneous pain is one of the most distressing features of arthritic conditions that reduces
254 the overall feeling of well-being (Hawker et al., 2008; Treharne et al., 2005) and it has been
255 suggested that burrowing and digging behaviors function as indicators of well-being in mice, such
256 that a reduction in burrowing behavior during inflammatory pain indicates diminished well-being
257 (Deacon, 2006; Jirkof, 2014). Based on this hypothesis, we measured digging behavior in a subset
258 of mice ($n = 7$, timeline Figure 1A, see Video, Supplementary Digital Content 1, which
259 demonstrates post-FB and post-CFA digging behavior of a mouse). During a 3-minute test period,
260 neither the time spent digging (pre-FB, 45.8 ± 5.9 s vs. post-FB, 39.8 ± 4.7 s, $F(1.8,11.3) = 9.8$, t
261 $(6) = 1.1$, ANOVA, Holm-Sidak's multiple comparison test, Figure 1D), nor the number of
262 burrows dug (pre-FB, 3.8 ± 0.3 vs. post FB, 3.7 ± 0.2, $F(1.7,10.4) = 21.8$, $t (6) = 0.5$, ANOVA,
263 Holm-Sidak's multiple comparison test, Figure 1E) was altered following FB injection. However,
264 CFA injection resulted in decreased digging time (pre-CFA, 52.7 ± 9.1 s vs. post-CFA, 17.9 ± 6.9

s, $F(1.8,11.3) = 9.8$, $t(6) = 3.9$, $p = 0.003$, ANOVA, Holm-Sidak's multiple comparison test, Figure 1D) and a decreased number of burrows dug (pre-CFA, 4.3 ± 0.2 vs. post-CFA, 2.1 ± 0.3, $F(1.7,10.4) = 21.8$, $t(6) = 6.3$, $p = 0.0003$, ANOVA, Holm-Sidak's multiple comparison test, Figure 1E), suggesting a significant impact to well-being, elicited by joint inflammation. Comparison of post-FB and post-CFA time points also showed that CFA-injection produced a reduction in the time spent digging ($F(1.8,11.3) = 9.8$, $t(6) = 4.8$, $p = 0.003$ ANOVA, Holm-Sidak's multiple comparison test) and in the number of burrows dug ($F(1.7,10.4) = 21.8$, $t(6) = 4.3$, $p = 0.0003$, ANOVA, Holm-Sidak's multiple comparison test).

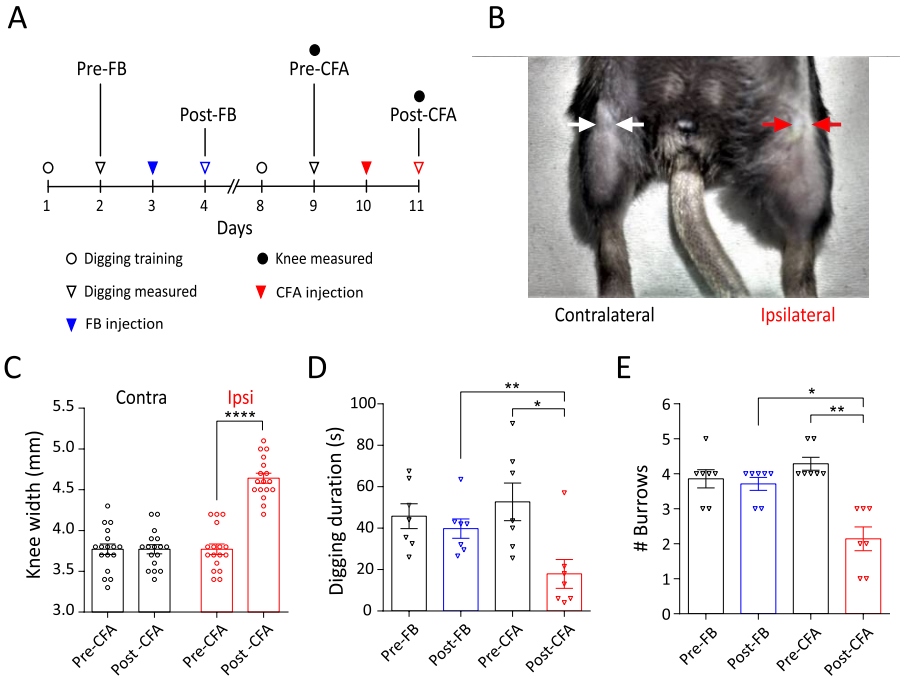

Figure 1: CFA model of acute knee inflammation in mice. A) Experimental timeline indicating when intra-articular injections, behavioral training and measurements were conducted. B) Representative picture of CFA injected (ipsilateral) and non-injected (contralateral) knee (shaved before injections). Arrows indicate where knee width was measured. C) Knee width on the day of CFA injection (pre) and 24-hours after CFA injection (post) in the ipsilateral (red dots) and contralateral (black dots) knee (n =17). **** indicates $p < 0.0001$, paired t-test. Plots of (D) time spent digging and (E) the number of visible burrows after a 3-minute digging test (n = 7). * indicates $p < 0.05$, ** indicates $p < 0.01$, repeated measures ANOVA, Holm-Sidak multiple comparison test. Error bars indicate SEM.

281 *3.2.Action potential threshold of knee neurons decreases after intra-articular CFA injection.*

282 To determine if altered sensory input may underlie the inflammation-induced decrease in
283 digging behavior observed, we characterized the electrical properties of knee-innervating DRG
284 neurons isolated from mice undergoing unilateral CFA knee injection as above (CFA neurons);
285 DRG neurons innervating the contralateral knee were used as control (Cntrl neurons). *In vivo*
286 recordings from rat joint afferents have shown increased excitability during inflammation (Grubb
287 et al., 1991). Therefore, we hypothesized that AP threshold would decrease in mouse knee neurons
288 following CFA-injection.

289 We recorded electrically-evoked APs from CFA neurons (Figure 2A) (CFA, n = 25) and
290 Cntrl neurons (n = 27) with similar diameters ($t(50) = 0.47$, $p = 0.6$, Figure 2B, Table 1) after 4-
291 hours in culture. The AP threshold of CFA neurons was ~ 30 % lower compared to Cntrl neurons
292 ($t(50) = 2.52$, $p = 0.01$, unpaired t-test) (Figure 2C, Table 1), suggesting hyperexcitability and
293 sensitization of these neurons. By contrast, there was no change in the HPD ($t(50) = 1.2$, $p = 0.3$,
294 unpaired t-test, Figure 2D), AHP amplitude ($t(50) = 1.9$, $p = 0.06$, Figure 2F) or amplitude ($t(50)$
295 $= 0.3$, $p = 0.7$, unpaired t-test, Table 1) of the electrically-evoked APs following inflammation,
296 whilst the AHP increased ($t(50) = 2.7$, $p = 0.009$, unpaired t-test, Figure 2E).

297

298

299

300

301

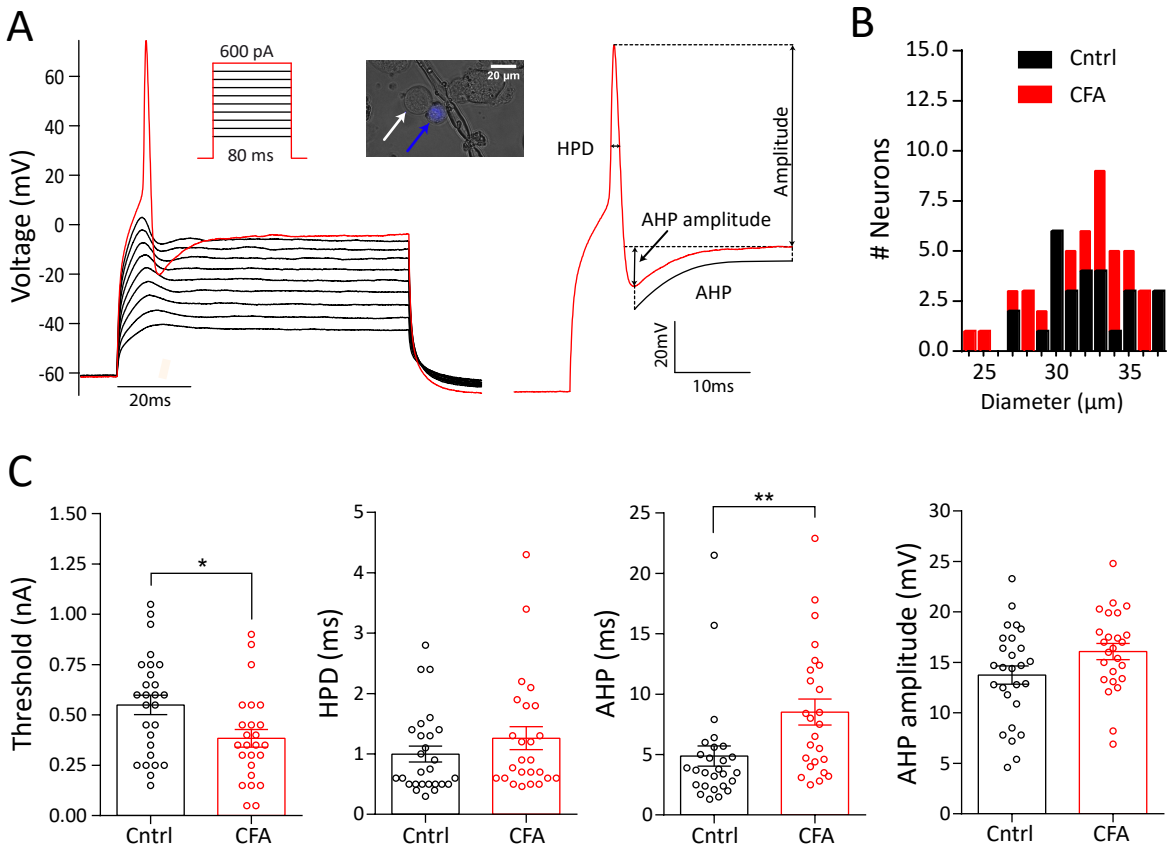

Figure 2: Action potential properties of knee neurons following acute knee inflammation. A) Action potential generation protocol (inset) and response along with a close-up of an evoked action potential from a knee neuron showing the different parameters measured. Example of a labeled knee neuron (blue arrow) and an unlabeled neuron (white arrow) shown in inset. Scale bar indicates 25 µm. B) Frequency distribution of neuronal diameter in µm of CFA (red, n = 25) and Cntrl (black, n = 27) neurons. C-F) Distribution of threshold (C), half peak duration (HPD) (D), afterhyperpolarization (AHP) (E) and AHP amplitude (F) after 4-hours in culture. Error bars indicate SEM, * indicates $p < 0.05$, ** indicates $p < 0.01$, unpaired t-test.

3.3.Acid-sensitivity does not change in knee neurons following inflammation.

Tissue acidosis occurs in some forms of inflammation in humans (Farr et al., 1985; Fujii et al., 2015), and in rodents there are also contrasting findings (Andersson et al., 1999; Wright et al., 2018). We used a range of pH solutions to determine if knee neuron acid-sensitivity changes following knee CFA injection. Depending upon the pH stimulus used, virtually all neurons responded with an inward current (pH 7 = 80.6 ± 4.6 %, pH 6 = 98.0 ± 2.0 % and pH 5 = 100 %,

316 combined percentage from CFA and Cntrl groups). A small proportion of neurons showed a
317 rapidly activating transient inward current followed by a sustained phase (transient + sustained) at
318 pH 6 and pH 5. These currents were likely mediated by acid-sensing ion channels (ASICs) and
319 their frequency was unaltered in CFA neurons (CFA, 16.3 ± 3.7 %; Cntrl, 11.1 ± 3.7 %, combined
320 mean of pH 6 and pH 5) (Figure 3A, 3B). Sustained currents were the dominant response at all
321 the pH tested (Figure 3A, C) and no difference was observed in the amplitude of response to any
322 pH stimulus between CFA and Cntrl neurons (Figure 3D-F, Table 2). Overall, this suggests that
323 there was no significant change in acid sensitivity in articular neurons during acute inflammation.

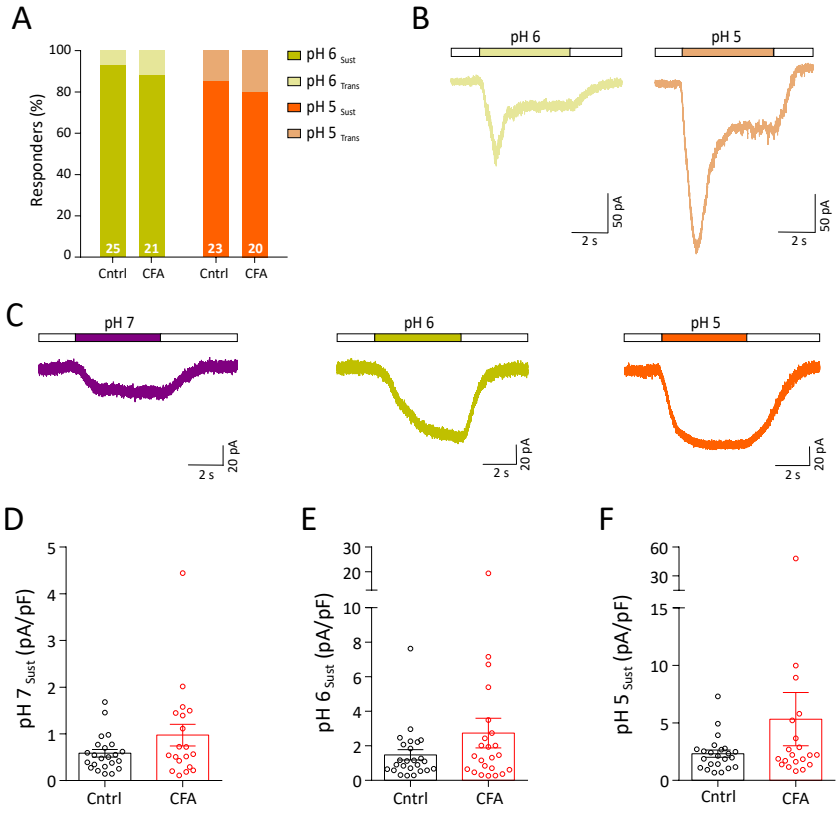

324

325 Figure 3: Acid sensitivity of knee neurons after acute inflammation. A) Percentage frequency of transient + sustained
326 vs. sustained only response to pH 6 (transient + sustained, light yellow; sustained, dark yellow) and pH 5 (transient +
327 sustained, light orange; sustained, orange) B) Example traces of transient + sustained acid currents in response to pH
328 6 (light yellow) and pH 5 (light orange). C) Example traces of sustained response to pH 7 (purple), pH 6 (dark yellow)
329 and pH 5 (orange). D-F) Peak current density of sustained pH 7, pH 6 and pH 5 responses (CFA: red dots, Cntrl:
330 black dots).

331 *3.4.Inflammation increases the proportion of TRPV1 expressing knee neurons.*

332 Sensory neurons express a variety of TRP channels involved in thermo- and chemosensing
333 and these are both activated and sensitized by a range of inflammatory mediators (Moore et al.,
334 2018). To determine if any change in TRP-mediated chemosensitivity occurs in knee neurons
335 following acute inflammation, we tested 10 μM capsaicin, 100 μM cinnamaldehyde and 100 μM
336 menthol, agonists of TRPV1, TRPA1 and TRPM8 respectively.

337 The percentage of capsaicin-sensitive CFA neurons increased significantly compared to
338 Cntrl neurons (CFA, 72 % vs. Cntrl, 44 %, $X^2(1) = 4.0$, $p = 0.04$, chi-sq test, Figure 4A). However,
339 there was no change in the peak current density of capsaicin-evoked currents ($t(28) = 1.0$, $p = 0.3$,
340 unpaired t-test, Table 2). By contrast, no change in the percentage of cinnamaldehyde-sensitive
341 (CFA, 40 %, Cntrl, 67 %, $X^2(1) = 3.7$, $p = 0.06$; chi-sq test, Figure 4B) or menthol-sensitive
342 neurons (CFA, 35 %, Cntrl, 51 %, $X^2(1) = 1.3$, $p = 0.2$, chi-sq test, Figure 4C) was observed, nor
343 was there any difference in the peak current density of either cinnamaldehyde- or menthol-evoked
344 currents following inflammation (Table 2, cinnamaldehyde, $t(26) = 0.6$, $p = 0.5$; menthol, $t(21) =$
345 0.2, $p = 0.9$, unpaired t-test). An increased proportion of knee DRG neurons responding to
346 capsaicin in inflammation suggests recruitment of a previously capsaicin "silent" population
347 (Figure 4D).

348 To confirm that an increase in the proportion of capsaicin sensitive knee neurons is due to
349 increased TRPV1 expression in knee neurons, we conducted immunohistochemistry on whole
350 DRG sections (L2-L5) from ipsilateral (CFA, n = 1089 neurons) and contralateral (Cntrl, n = 1334
351 neurons) sides of four mice (Figure 4Ei). A significantly higher proportion of CFA neurons
352 displayed TRPV1 expression (59.7%) compared to Cntrl neurons (44.6 %, $X^2(1) = 48.03$, $p <$
353 0.0001, chi-sq test, Figure 4Eii). Nerve growth factor (NGF) is an important inflammatory

354 mediator implicated in arthritis that binds to its high affinity receptor tropomyosin receptor kinase
355 A (TrkA) and can increase TRPV1 expression (Ji et al., 2002). Hence, we hypothesized that the
356 increased TRPV1 expression observed will occur in TrkA positive neurons, leading to increased
357 TRPV1 and TrkA coexpression. Although, the proportion of knee neurons expressing TrkA (CFA,
358 39.3 %, Cntrl, 42.6 %) (Figure 4Eii) was not greater in CFA neurons than Cntrl neurons, there was
359 a small, yet significant, increase in the proportion of CFA neurons co-expressing TRPV1 and TrkA
360 compared to Cntrl neurons (CFA, 24.8 %; Cntrl, 29.8 %, $X^2(1) = 5.6$, $p = 0.02$, chi-sq test, Figure
361 4Eii). Taken together, our data suggests that NGF-TrkA signaling contributes, alongside as yet
362 unknown pathways, to driving increased TRPV1 expression following CFA.

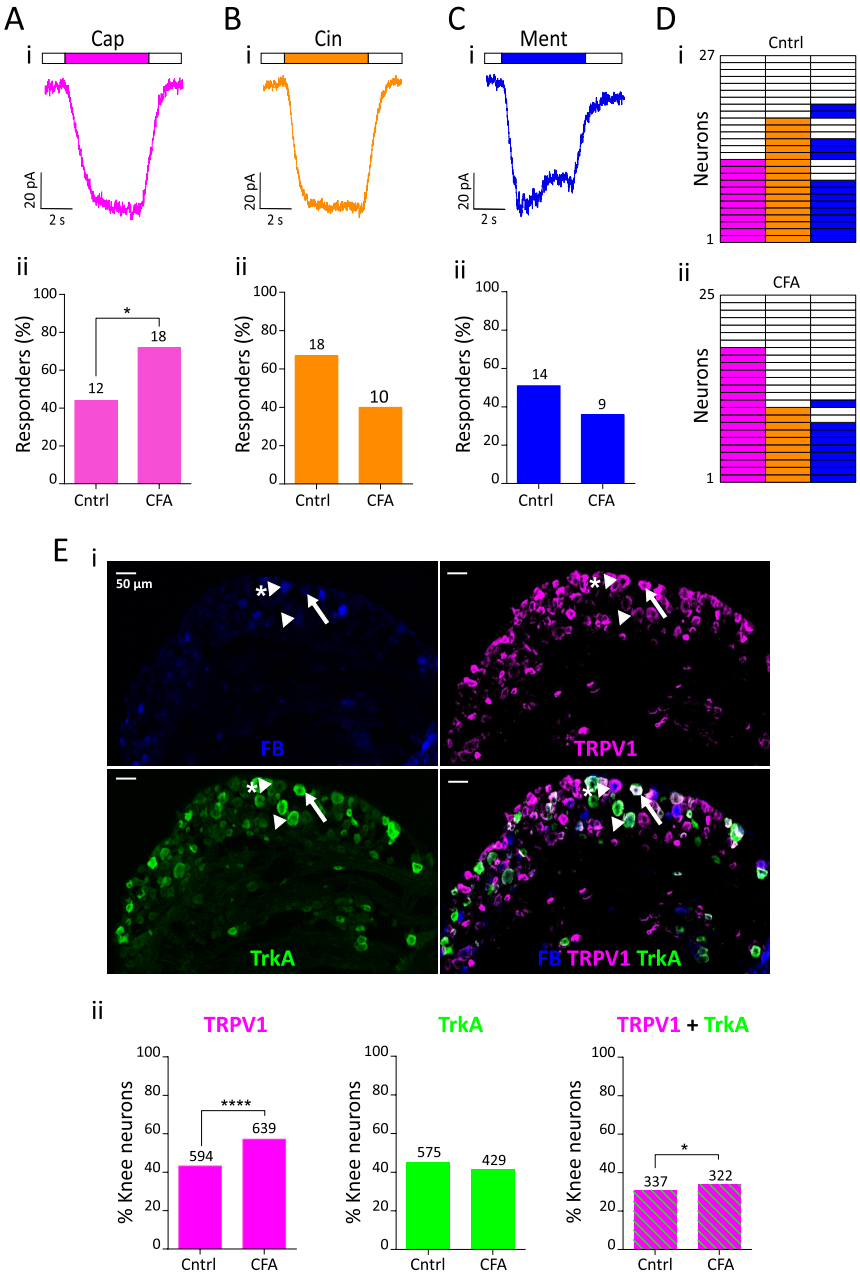

Figure 4: TRP agonist response profile of knee neurons following acute knee inflammation. Representative traces of 10 µM capsaicin (pink, Ai), 100 µM cinnamaldehyde (orange, Bi) and 100 µM menthol (blue, Ci) response from a CFA neuron and their respective percentage frequency (Aii, Bii, Cii). The numbers above the bars indicate the number of responsive neurons. D) Heat map of Cntrl (i, n = 27) and CFA (ii, n = 25) neurons responding to capsaicin, cinnamaldehyde and menthol. E (i) Representative images of a whole DRG section from L4 showing fast blue (FB) labeling from the knee (blue), TRPV1 expression (pink), TrkA expression (green) and a merged image; sections from an animal injected with CFA. White arrowhead shows a knee neuron that only expresses TrkA, white arrowhead with asterisk shows a knee neuron that expresses only TRPV1 and white arrow shows a knee neuron that co-expresses TRPV1 and TrkA. (ii) Proportion of knee neurons (L2-L5) that express TRPV1 (pink), TrkA (green) and both TRPV1 and TrkA (green and pink stripes) from Cntrl (n = 1334) and CFA (n = 1089) injected side. Numbers above the bars represent neurons stained positive with respective antibodies. * indicates $p < 0.05$, **** indicates $p < 0.0001$, chi-sq test.

376 *3.5.Sustained $GABA_A$-evoked current magnitude increases in knee neurons following*
377 *inflammation.*

378 An inflammation-induced increase in amplitude of GABA-evoked currents has been
379 reported in skin-labeled rat DRG neurons, suggesting that altered GABAergic signaling may be
380 important in inflammatory pain (Zhu et al., 2012). Two types of GABA response were observed.
381 In the first, the current reached a peak within 1.5 s of GABA application and was classified as
382 transient + sustained (TS). Two subtypes of TS responses were observed: one showing relatively
383 monophasic desensitization throughout GABA application (Figure 5Ai) and a second showing a
384 far slower desensitization that produced a more stable sustained phase (Figure 5Aii); due to the
385 paucity of neurons in the first subgroup and since no response returned to baseline within 5 s, both
386 types were included in the TS group. The second type of GABA-evoked response did not reach its
387 peak within the first 1.5 s, showed no desensitization and was classified as sustained (S, Figure
388 5Aiii). The frequency of TS and S responses in CFA and Cntrl neurons was similar (CFA: TS, 48
389 %, S, 28 % vs. Cntrl: TS, 52 %, S, 44 %, Figure 5 Bi). We also observed that 100 μM GABA
390 evoked a response in 76 % of CFA and 96 % of Cntrl neurons ($X^2(1) = 4.6$, $p = 0.03$, chi-sq test,
391 Figure 5 Bi). Although no difference in GABA-evoked peak current density was observed overall
392 between CFA and Cntrl neurons (Figure 5Bii, Table 2), GABA-evoked S type currents were of
393 larger magnitude in CFA than Cntrl neurons (CFA, 8.0 ± 4.1 pA/pF, n =7 vs. Cntrl, 1.7 ± 0.6
394 pA/pF, n = 14, $t(19) = 2.1$, $p = 0.04$, unpaired t-test), whereas no such difference was observed for
395 TS type currents (CFA, 6.7 ± 2.4 pA/pF, n =12 vs. Cntrl, 6.5 ± 1.9, n = 12, $t(22) = 0.05$, $p = 0.9$,
396 unpaired t-test) (Figure 5Biii).

397 Due to inflammation producing an increase in the magnitude of S type GABA-evoked
398 currents, we investigated the subunit composition of these GABA receptors. The $GABA_A$

399 antagonist, bicuculline, inhibited GABA responses by more than 50 % in 6/7 CFA DRG and 8/12
400 Cntrl DRG (Figure 5Ci), with all GABA-evoked currents being sensitive to bicuculline to some
401 extent. These results concur with the previous observation that a fraction of GABA-evoked
402 currents in rat DRG neurons is bicuculline insensitive (Lee et al., 2012). S type $GABA_A$ currents
403 can be mediated by δ subunit containing $GABA_A$ receptors (Lee et al., 2012) and thus we tested
404 the ability of the δ subunit containing $GABA_A$ receptor agonist THIP to evoke currents in knee
405 neurons. A sustained current in response to THIP was observed in 4/8 CFA and 6/11 Cntrl neurons,
406 indicating expression of δ-subunit containing $GABA_A$ receptors in knee neurons (Figure 5Ci, Cii).
407 The peak current density of THIP-evoked currents was similar ($t(8) = 0.18$, $p = 0.9$, unpaired t-
408 test) in CFA (0.6 ± 0.2 pA/pF) and Cntrl (0.5 ± 0.1 pA/pF) neurons. However, not all the neurons
409 with S type GABA response showed THIP sensitivity. Combined with the presence of bicuculline
410 insensitive currents, the lack of response to THIP in all neurons with S currents suggests expression
411 of either ρ subunit containing $GABA_A$ receptors, or perhaps $GABA_B$ receptors, both of which
412 produce sustained currents in response to GABA (Chebib and Johnston, 2001). Taken together,
413 our data indicate the presence of diverse $GABA_A$ receptor subunits in CFA and Cntrl neurons and
414 demonstrate an increase in GABA-mediated neuronal excitation following knee inflammation.

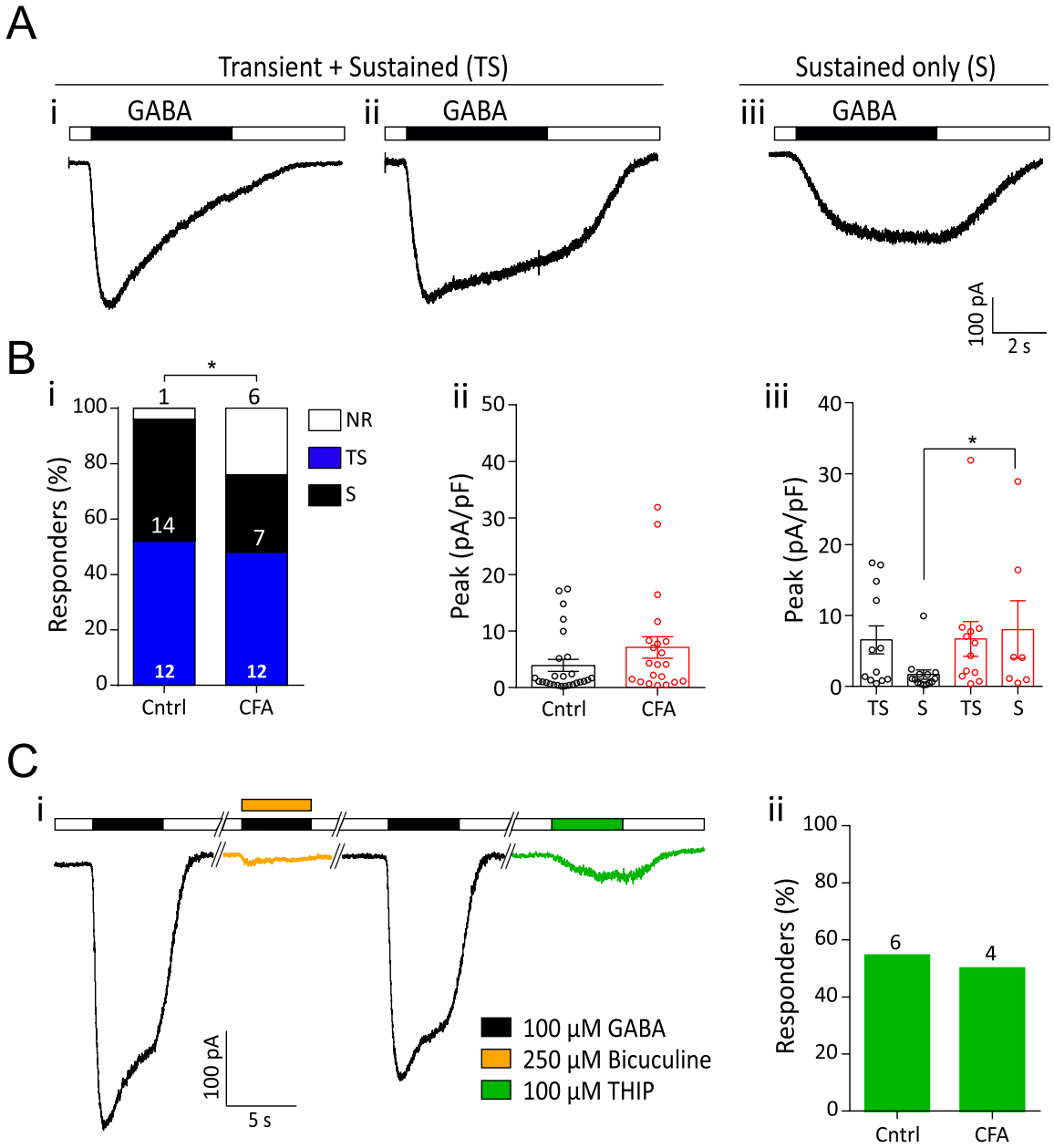

Figure 5: GABA-evoked currents from knee neurons after acute inflammation. A) Representative traces of 100 µM GABA-evoked currents showing both transient and sustained phases (i, ii) and currents with only a sustained phase (iii). B (i) Percentage frequency of GABA-evoked transient + sustained currents (blue bars), sustained currents (black bars) and non-responders (white bars) in Cntrl and CFA neurons. (ii) Peak current density of all GABA-evoked currents (Cntrl: n = 26, CFA: 19) and (iii) GABA-evoked currents split into TS and S type (Cntrl: black dots; CFA: red dots). TS = transient + sustained currents, S = sustained only currents, error bars indicate SEM, * indicates $p < 0.05$, unpaired t-test. C) i - Example trace of bicuculline block (yellow) of GABA-evoked currents and THIP-evoked current (green) in a single neuron. ii – percentage frequency of Cntrl (n = 11) and CFA (n = 8) neurons with a GABA response that also responded to THIP. The numbers above the bars indicate the number of responsive neurons.

3.6. *Time-in-culture leads to loss of inflammation-induced sensitization of knee neurons.*

The period of time that neurons are left in culture for (time-in-culture) and constituents of the culture medium can greatly alter neuronal excitability (Scott and Edwards, 1980; Winter et al., 1988). To systematically characterize the effect of time-in-culture in our system, we repeated the experiments described above on the CFA and Cntrl knee neurons after 24-hours (CFA, n = 25; Cntrl, n = 22) and 48-hours (CFA, n = 23; Cntrl, n = 22) in culture.

No change was observed in the resting membrane potential, capacitance or AP amplitude (Table 1) across the three time points. By contrast, whereas the AP threshold was similar across time points for CFA knee neurons ($F(2,70) = 2.4$, $p = 0.09$, ANOVA), it decreased for Cntrl neurons after 48-hours in culture compared to 24-hours ($F(2,68) = 3.4$, $t(68) = 2.6$, $p = 0.03$, ANOVA, Holm-Sidak multiple comparison test, Table 1). Interestingly, the inflammation-induced decrease in AP threshold of CFA neurons compared to Cntrl neurons that was observed at 4-hours (Figure 2C) and 24-hours ($t(45) = 3.3$, $p = 0.002$, unpaired t-test, Table 1) had disappeared after 48-hours in culture (Table 1, $t(43) = 0.8$, $p = 0.44$, unpaired t-test), which suggests that time-in-culture leads to a loss of inflammation-induced hyperexcitability. There was also a distinct AP widening characterized by an increase in both HPD and AHP in the 48-hours group for Cntrl neurons, but just the HPD in CFA neurons. HPD increased by ~ 60 % after 48-hours in both CFA ($F(2,70) = 2.4$, $t(70) = 2.3$, $p = 0.01$, ANOVA, Holm-Sidak multiple comparison test) and Cntrl ($F(2,68) = 8.1$, $t(68) = 4.0$, $p = 0.007$, ANOVA, Holm-Sidak multiple comparison test) neurons compared to the 4-hours group (Table 1). In Cntrl neurons, AHP increased by 191 % in the 48-hours group compared to 4-hours and 81 % compared to 24-hours group ($F(2,68) = 10.0$, $p = 0.0002$, ANOVA, Holm-Sidak multiple comparison test, Table 1). One CFA and one Cntrl neuron

447 in the 48-hours culture group were excluded from this analysis because of a highly different AP
448 waveform that could not be analyzed using the same measurements.

449 With regards to knee neuron acid sensitivity, the percentage of neurons with transient +
450 sustained currents in response to pH 6 and pH 5 at 24-hours and 48-hours (see Figure,
451 Supplementary Digital Content 2A showing time-in-culture effects on acid of knee neurons after
452 inflammation) was similar to that at 4-hours (Figure 3A). Although a largely reversible increase in
453 pH 7- (CFA and Cntrl) and pH 5-evoked (Cntrl) current amplitude was observed at 24-hours (pH
454 7: CFA, $F(2,50) = 5.7$, $p = 0.005$; Cntrl, $F(2,52) = 9.3$, $p = 0.0003$; pH 6: CFA, $F(2,65) = 2.8$, $p =$
455 0.06; Cntrl, $F(2,60) = 2.6$, $p = 0.08$; and pH 5: CFA, $F(2,57) = 2.8$, $p = 0.06$; Cntrl, $F(2,54) = 5.2$,
456 $p = 0.008$, ANOVA) (Table 2), there was no clear trend across different pH stimuli for either CFA
457 or Cntrl neurons.

458 For knee neuron TRP-mediated chemosensitivity, the CFA-induced increase in the
459 proportion of capsaicin-sensitive neurons observed at 4-hours was maintained at 24-hours (CFA,
460 88 % vs. Cntrl, 50%, $X^2(1) = 8.1$, $p = 0.004$, chi-sq test), but was absent in the 48-hours group
461 (CFA, 54.2 % vs. Cntrl, 43.5 %, $X^2(1) = 0.5$, $p = 0.5$, chi-sq test), a result that further confirms our
462 observations that after 48-hours in culture the inflammation-induced effects are lost. In addition,
463 the proportion of cinnamaldehyde (CFA, 33.3 %; Cntrl, 21.7 %) and menthol-sensitive (CFA, 33.3
464 %; Cntrl, 13.0 %) neurons after 48-hours in culture decreased compared to the other two time
465 points, although this decrease was only significant in Cntrl neurons (cinnamaldehyde, $X^2(1) =$
466 11.9, $p = 0.0006$; menthol, $X^2(1) = 7.8$, $p = 0.005$, chi-sq test) (see Figure, Supplementary Digital
467 Content 2B, showing time-in-culture effects on TRP agonist of knee neurons after inflammation).
468 No significant difference in the peak current density of TRP agonist-evoked currents was observed
469 across time-in-culture (Table 2).

470 When GABA-evoked currents were split into TS and S types, no changes in the peak
471 current density were observed between CFA and Cntrl after 24-hours or 48-hours in culture.
472 However, combining both TS and S currents, CFA neurons had larger amplitude GABA-evoked
473 currents than Cntrl neurons after 24-hours in culture ($t(39) = 2.5$, $p = 0.01$, unpaired t-test, Table
474 2); an effect that was not seen in the 48-hours group ($t(32) = 1.2$, $p = 0.2$, unpaired t-test, Table 2).
475 Previously, it has been shown in cultured rat DRG neurons that the proportion of S type GABA-
476 evoked currents increased with time-in-culture (Lee et al., 2012), a result replicated here in mouse
477 knee neurons (CFA, $X^2(1) = 4.8$, $p = 0.03$, Cntrl, $X^2(1) = 5.4$, $p = 0.02$, chi-sq test, see Figure,
478 Supplementary Digital Content 2C, showing time-in-culture effects on GABA sensitivity of knee
479 neurons after inflammation). From this data, we would recommend not using DRG neurons for
480 longer than 28-hours in culture to prevent loss of inflammation-induced sensitization events.

481

482 *3.7.TRPV1 inhibition reverses inflammation induced decrease in digging behavior.*

483 From our characterization of CFA and Cntrl neurons, knee neuron TRPV1 expression
484 emerged as an important target in CFA-induced knee inflammation. We hypothesized that TRPV1
485 underlies our observed knee inflammation-induced decrease in digging behavior observed in mice
486 and that the TRPV1 antagonist A-425619 would thus reverse this decrease. On day 2 of our
487 experimental timeline (Figure 6A), both the CFA group ($n = 10$) and saline group ($n = 7$) spent a
488 similar amount of time digging (CFA, 31.1 ± 6.1 s; Saline, 33.8 ± 6.4 s) and produced a similar
489 number of burrows (CFA, 4.3 ± 0.4; Saline, 3.4 ± 0.4) during a 3 min test in the digging cage.
490 Following CFA/saline injection, the CFA group showed an expected decrease in digging duration
491 (17.4 ± 5.2 s, $F(1.8,16.6) = 10.1$, $t(9) = 3.6$, $p = 0.001$, repeated measures ANOVA, Holm-Sidak
492 multiple comparison test, Figure 6B), which was reversed 30 min after the injection of A-425619

493 (36.4 ± 7.0 s, $F(1.8,16.6) = 10.1$, $t(9) = 3.9$, $p = 0.001$, ANOVA, Holm-Sidak multiple comparison
494 test, Figure 6B). A similar result was also obtained with the number of burrows (post-CFA, 2.1 ±
495 0.3, $F(1.9,17.9) = 18.9$, $t(9) = 5.0$; post-Ant, 4.0 ± 0.2, $F(1.9,17.9) = 18.9$, $t(9) = 5.0$, $p < 0.0001$,
496 repeated measures ANOVA, Holm-Sidak multiple comparison test, Figure 6C). In contrast, the
497 saline group did not show a decrease in digging behavior 24-hours after saline injection into the
498 knee (Digging duration, 33.1 ± 5.3 s, $F(1.5,9.0) = 0.6$, $t(6) = 0.1$, $p = 0.5$; # Burrows, 3.7 ± 0.5,
499 $F(1.7,10.0) = 0.3$, $t(6) = 0.6$, $p = 0.7$, repeated measures ANOVA, Holm-Sidak multiple
500 comparison test, Figure 6D, 6E), further confirming that intra-articular injections do not affect
501 digging behavior. The TRPV1 antagonist A-425619 also produced no effect on digging behavior
502 in the saline group (Digging duration, 25.9 ± 6.3 s, $F(1.5,9.0) = 0.6$, $t(6) = 0.8$, $p = 0.5$; # Burrows,
503 3.3 ± 0.4, $F(1.7,10.0) = 0.3$, $t(6) = 0.6$, $p = 0.7$, ANOVA, Figure 6D, 6E), i.e. inhibiting TRPV1
504 does not interfere with spontaneous digging activity of mice. These results confirm that TRPV1 is
505 an important mediator of inflammatory knee pain and contributes to the inflammation-induced
506 decrease in digging behavior in mice.

507

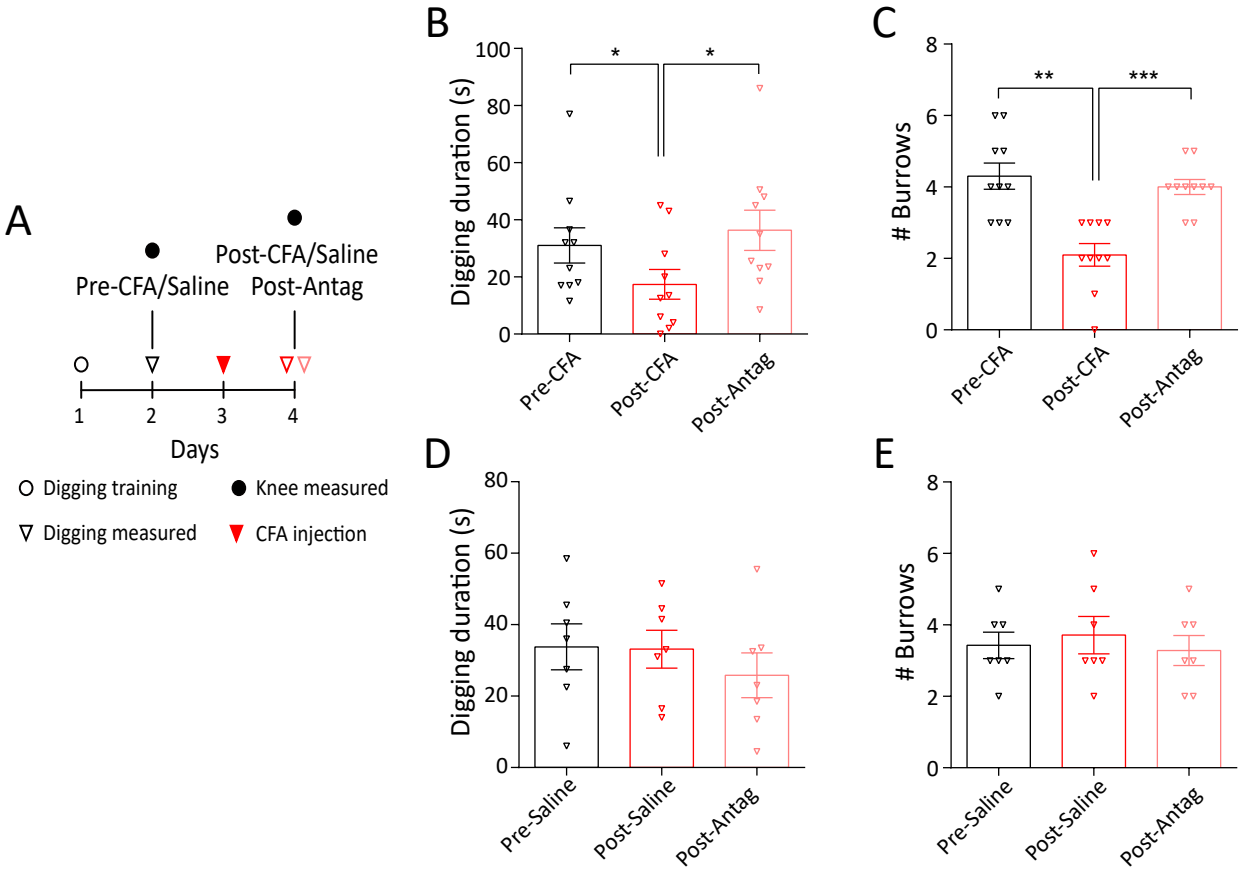

Figure 6: Digging behavior after injection of the TRPV1 antagonist A-425619. A) Experimental timeline highlighting the days where behavioral testing and injection was performed. Distribution of time spent digging and the number of burrows in the CFA (B, C, n = 10) and saline group (D, E, n = 7). * indicates $p < 0.05$, ** indicates $p < 0.01$, *** indicates $p < 0.0001$. rmANOVA, Holm-Sidak multiple comparison test. Error bars indicate SEM.

4. Discussion

CFA evokes both acute (within 18 hours) and chronic (> 6 weeks) inflammatory pain (Hsieh et al., 2017; Keeble et al., 2005), as demonstrated by altered evoked-pain behaviors, such as hot/cold plate tests. However, such evoked-pain tests are neither ethologically relevant to rodents, nor model experience of human chronic pain (Rice et al., 2008). Consequently, innate rodent behaviors, such as burrowing, digging and nest-building that seek to mirror human activities of daily living have been explored as pain assays (Deacon, 2006; Jirkof, 2014; Shepherd et al., 2018). A decrease in burrowing behavior has been used to assess pain-like behavior after CFA-

521 induced knee inflammation in rats (Rutten et al., 2014) and digging is a similar innate behavior
522 that is quick and easy to test in a laboratory (Deacon, 2006). Here we show that 24-hours after
523 CFA-induced knee inflammation, mice spent significantly decreased time digging, suggesting that
524 digging can be used as an ethologically relevant pain assay in mice; importantly, intra-articular
525 injection of the retrograde tracer FB did not alter digging behavior.

526 To study the neural basis for the inflammation-induced change in behavior observed, we
527 combined electrophysiology with retrograde labelling of the knee joints, i.e. those neurons exposed
528 to the inflammatory insult. We found that knee neurons have a decreased AP threshold and
529 increased AHP (although no change in AHP amplitude) following CFA-induced knee
530 inflammation. The recorded increased AHP in CFA neurons is perhaps contradictory because an
531 increase in current mediated by hyperpolarization-activated cyclic nucleotide-gated ion channels
532 (HCN), and thus a decrease in AHP, is associated with repetitive firing, as shown by one study in
533 trigeminal ganglia neurons after CFA-induced inflammation (Flake and Gold, 2005). However,
534 other studies using CFA-induced hind limb inflammation either observed no change in AHP (like
535 our data at 24-hours in culture) (Djouhri and Lawson, 1999) or reported a decrease in AHP only
536 in C-fibers (Weng et al., 2012). Therefore, our data possibly demonstrates the multifaceted nature
537 of the molecular mechanisms regulating AHP, a suggestion supported by the wide range of AHP
538 values reported (Djouhri et al., 1998; Lawson et al., 1996).

539 TRP channels are cellular sensors of thermal, physical and chemical stimuli (Moore et al.,
540 2018) and inflammatory mediators released during joint pain can sensitize TRP channels (Zhang
541 et al., 2013). TRPV1 (Zhang et al., 2005), TRPA1 (Story et al., 2003) and TRPM8 (Behrendt et
542 al., 2004) are expressed in nociceptors and are involved in hyperalgesia. However, the role of
543 TRPV1 and TRPA1 in acute inflammatory joint pain is unclear. Some studies report that TRPV1^{-}

544 $^{/-}$ mice do not develop CFA- (Keeble et al., 2005) or carrageenan- (Davis et al., 2000) induced
545 hyperalgesia and others have shown that in DRG neurons TRPV1 protein expression increases in
546 CFA-induced inflammation (Amaya et al., 2003; Ji et al., 2002; Yu et al., 2008). In direct contrast,
547 other studies failed to show increased neuronal TRPV1 protein (Bär et al., 2004; Zhou et al., 2003)
548 or mRNA expression (Ji et al., 2002) following CFA-induced inflammation. Similarly, TRPA1$^{-/-}$
549 mice show normal development of CFA-induced hyperalgesia in some studies (Fernandes et al.,
550 2011; Petrus et al., 2007), whereas others report attenuation of CFA- and carrageenan-induced
551 hyperalgesia in TRPA1$^{-/-}$ mice (Garrison and Stucky, 2014; Moilanen et al., 2012) or following
552 administration of a TRPA1 antagonist (Bonet et al., 2013; Samer R Eid et al., 2008). We provide
553 electrophysiological evidence that the proportion of capsaicin-sensitive knee neurons increases
554 during acute inflammation from ~ 50% to ~80%, suggesting recruitment of a previously silent
555 neuronal population. We validate this electrophysiology result through immunohistochemistry,
556 demonstrating a similar magnitude increase in the proportion of TRPV1 expressing knee neurons;
557 the observed TRPV1 expression in contralateral knee-innervating neurons reported here agrees
558 with previous findings in rodents (Cho and Valtschanoff, 2008). Following that, we were able to
559 reverse the inflammation-induced reduction in digging behavior in mice by systemic
560 administration of the TRPV1 antagonist, A-425619, which suggests that the increased TRPV1
561 expression observed at the cellular level drives the pain behaviors. Multiple mechanisms may
562 contribute to the increase in TRPV1 expression, for example, NGF released from a variety of cell
563 types in arthritic joints may bind to TrkA and get retrogradely transported to DRG neurons to drive
564 TRPV1 expression. Indeed, increased levels of NGF are found in rheumatic diseases and anti-
565 NGF/TrkA therapy reduces arthritic pain in human and animal models (reviewed in (Seidel et al.,
566 2013)). With regard to CFA-induced pain, it has been previously shown that the proportion of

567 TrkA-expressing neurons innervating bone does not increase following CFA-induced bone pain
568 (Sara Nencini et al., 2017). We also observed no change in TrkA expression, but did observe a
569 slight, yet significant, increase in TrkA-TRPV1 co-expression following knee inflammation which
570 suggests that NGF-TrkA signaling plays a role in the increased TRPV1 expression observed here.

571 Protons are algogens detected by sensory neurons through a variety of means, including
572 ASICs, TRPV1, background K^+ channels, chloride channels and proton-sensing G-protein coupled
573 receptors (Holzer, 2009). There is conflicting evidence surrounding the role of ASICs in
574 inflammatory pain, some studies showing no change, others decreased pain and still others
575 increased pain (Price et al., 2001; Sluka et al., 2003). In terms of joint inflammation, $ASIC3^{-/-}$,
576 $TDAG8^{-/-}$ (a proton-sensing GPCR) and $TRPV1^{-/-}$ mice showed decreased hyperalgesia in an ankle
577 inflammation model (Hsieh et al., 2017). In addition, Ikeuchi *et al* (Ikeuchi et al., 2009) observed
578 upregulation of ASIC3 immunoreactivity in knee-innervating DRG neurons after carrageenan-
579 induced acute knee inflammation in mice. By contrast, ASIC1, ASIC2 and ASIC3 knockout mice
580 did not display attenuated thermal or mechanical hyperalgesia after intraplantar CFA injection,
581 suggesting that these ASIC subunits play no role in cutaneous CFA-induced hyperalgesia
582 (Staniland and McMahon, 2009). We evaluated direct proton activation of knee neurons and found
583 that acid-evoked currents are neither enhanced, nor is there any change in the proportion of ASIC-
584 like currents, following CFA-induced knee inflammation, results that might explain the lack of
585 phenotype observed in certain studies.

586 Information transfer from peripheral to central afferents is modulated by GABAergic
587 signaling. Although an inhibitory neurotransmitter in the central nervous system, GABA produces
588 membrane depolarization through Cl^- efflux in DRG neurons owing to the relatively high
589 intracellular $[Cl^-]$ (Sung et al., 2000). GABA-evoked currents in sensory neurons are

590 predominantly $GABA_A$ receptor mediated, (identified by their sensitivity to $GABA_A$ antagonist,
591 bicuculline) with diverse subunit composition (Lee et al., 2012). As shown previously in rat DRG
592 neurons (Lee et al., 2012), we recorded both transient and sustained GABA-evoked currents from
593 mouse knee neurons that were largely inhibited by the $GABA_A$ antagonist bicuculline. In addition,
594 our finding that approximately half of all knee neurons were activated by the $GABA_A$-δ subunit
595 agonist, THIP, suggests common expression of the δ-subunit, although the proportion of THIP-
596 activated neurons did not change after CFA injection. The fact that bicuculline did not completely
597 abolish GABA-evoked currents indicates the likely presence of ρ subunits in $GABA_A$ receptors,
598 as has previously been reported in rat DRG neurons (Lee et al., 2012), or the presence of $GABA_B$
599 receptor expression (both ρ containing $GABA_A$ receptors and $GABA_B$ receptors are insensitive to
600 bicuculline block). Under normal conditions, GABA-mediated excitation of primary afferent
601 neurons causes primary afferent depolarization, an inhibitory action due to inducing inactivation
602 of voltage gated sodium channels (i.e. depolarizing block). However, following tissue injury,
603 primary afferent depolarization is larger and can actually generate AP to produce pain by excitation
604 of presynaptic $GABA_A$ receptors (Cervero et al., 2003; Willis, 1999). In this study, we found a
605 decrease in number of GABA responsive CFA neurons, but an increase in the magnitude of
606 GABA-evoked currents compared to Cntrl neurons indicating a potential $GABA_A$ mediated
607 decrease in presynaptic inhibition and an increase in presynaptic excitation.

608 Furthermore, we addressed how time-in-culture affects the electrophysiological properties
609 of neurons isolated from mice undergoing CFA-induced inflammation. Acutely dissociated DRG
610 neurons have been extensively studied with patch clamp electrophysiology, however the definition
611 of "acute" varies. While some studies have recorded within 8-hours of dissection, it is more
612 common to record after overnight incubation (18–28-hours). This variability can potentially

613 confound results on inflammation-induced sensitization, as AP properties change with time-in-
614 culture. Here we show AP broadening, and a slight decrease in AP threshold in neurons from the
615 contralateral side as reported before during a similar time course (Scott and Edwards, 1980). We
616 also show that time-in-culture does not affect inflammation-induced lowering of AP threshold up
617 to 28-hours in culture, but that the lowered threshold is lost at 48-hours in culture. Understanding
618 how time-in-culture alters neuronal excitability is important for correctly designing studies. For
619 example, we (present study) and others (Lee et al., 2012) have shown that S type GABA-evoked
620 responses increase in prevalence with time-in-culture. The present study also shows a decline in
621 the frequency of response to capsaicin, cinnamaldehyde and menthol and the inflammation-
622 induced increase in frequency of capsaicin-sensitive neurons, although maintained for up to 28-
623 hours in culture is lost after 48-hours. By contrast, acid-sensitivity remained relatively stable across
624 all time points.

625 In summary, we show that following unilateral acute inflammation of the knee, knee
626 neurons have 1) a lower AP threshold 2) increased sensitivity to capsaicin and expression of
627 TRPV1 and 3) an increasing trend in the magnitude of GABA-evoked currents up to 28-hours in
628 culture. This specific sensitization signature of knee neurons highlights the importance of studying
629 DRG neurons as a spatially heterogeneous group. Among these different modes of sensitization
630 that likely contribute to the decreased mouse digging behavior following knee inflammation, an
631 increase in TRPV1 function is perhaps most clinically relevant to inflammatory arthritis (reviewed
632 in (Fernandes et al., 2013). Indeed, it has recently been shown that intra-articular administration
633 of a TRPV1 antagonist attenuated early osteoarthritic pain in a mono-sodium iodoacetate model
634 of osteoarthritis (Haywood et al., 2018). Historically in pre-clinical models, TRPV1 antagonists
635 attenuated thermal hyperalgesia, but their efficacy in mechanical hyperalgesia and ongoing pain is

636 unclear (Brandt et al., 2012). The peripherally restricted TRPV1 antagonist, A-425619, has been
637 previously shown to reverse thermal and mechanical hypersensitivity in rat CFA models and also
638 restore weight bearing ability in rat osteoarthritis models (Honore et al., 2005). Here we report that
639 systemic administration of A-425619 is also able to restore the reduction in spontaneous digging
640 behavior in mice brought about by CFA-induced knee inflammation, which further establishes
641 TRPV1 as an important drug target in inflammatory joint pain.

642

643 Declaration of Interest

644 The authors declare no conflict of interest regarding information in the present report.

645 Acknowledgments

646 The authors would like to thank Julie Gautrey and Chris Cardinal for technical assistance with
647 animal work. This work was supported by an Arthritis Research UK Grant (G.C. and E.St.J.S., RG
648 20930), a Rosetrees Postdoctoral Grant (J.R.F.H. and E.St.J.S., A1296), S.C. was supported by a
649 Gates Cambridge Trust scholarship and L.A.P. was supported by the University of Cambridge
650 BBSRC Doctoral Training Programme (BB/M011194/1).

651 Data Statement

652 The datasets presented in this study can be accessed from the University of Cambridge Apollo data
653 repository (https://doi.org/10.17863/CAM.24492).

654

655

656

References

Amaya, F., Oh-hashi, K., Naruse, Y., Iijima, N., Ueda, M., Shimosato, G., Tominaga, M., Tanaka, Y., Tanaka, M., 2003. Local inflammation increases vanilloid receptor 1 expression within distinct subgroups of DRG neurons. Brain Research 963, 190–196. https://doi.org/10.1016/S0006-8993(02)03972-0

Andersson, S.E., Lexmuller, K., Johansson, A., Ekstrom, G.M., 1999. Tissue and intracellular pH in normal periarticular soft tissue and during different phases of antigen induced arthritis in the rat. J Rheumatol 26, 2018–2024.

Arendt-Nielsen, L., 2017. Joint pain: more to it than just structural damage? PAIN 158.

Bär, K.-J., Schaible, H.-G., Bräuer, R., Halbhuber, K.-J., von Banchet, G.S., 2004. The proportion of TRPV1 protein-positive lumbar DRG neurones does not increase in the course of acute and chronic antigen-induced arthritis in the knee joint of the rat. Neuroscience Letters 361, 172–175. https://doi.org/10.1016/j.neulet.2003.12.034

Behrendt, H.-J., Germann, T., Gillen, C., Hatt, H., Jostock, R., 2004. Characterization of the mouse cold-menthol receptor TRPM8 and vanilloid receptor type-1 VR1 using a fluorometric imaging plate reader (FLIPR) assay. British Journal of Pharmacology 141, 737–745. https://doi.org/10.1038/sj.bjp.0705652

Bonet, I.J.M., Fischer, L., Parada, C.A., Tambeli, C.H., 2013. The role of transient receptor potential A 1 (TRPA1) in the development and maintenance of carrageenan-induced hyperalgesia. Neuropharmacology 65, 206–212. https://doi.org/10.1016/j.neuropharm.2012.09.020

Bonin, R.P., Zurek, A.A., Yu, J., Bayliss, D.A., Orser, B.A., 2013. Hyperpolarization-Activated Current (Ih) Is Reduced in Hippocampal Neurons from Gabra5−/− Mice. PLOS ONE 8, e58679. https://doi.org/10.1371/journal.pone.0058679

Brandt, M.R., Beyer, C.E., Stahl, S.M., 2012. TRPV1 Antagonists and Chronic Pain: Beyond Thermal Perception. Pharmaceuticals 5, 114–132. https://doi.org/10.3390/ph5020114

Caceres, A.I., Liu, B., Jabba, S.V., Achanta, S., Morris, J.B., Jordt, S., 2017. Transient Receptor Potential Cation Channel Subfamily M Member 8 channels mediate the anti-inflammatory effects of eucalyptol. British Journal of Pharmacology 174, 867–879. https://doi.org/10.1111/bph.13760

Cervero, F., Laird, J.M.A., García-Nicas, E., 2003. Secondary hyperalgesia and presynaptic inhibition: an update. European Journal of Pain 7, 345–351. https://doi.org/10.1016/S1090-3801(03)00047-8

Chebib, M., Johnston, G.A.R., 2001. The “ABC” of GABA receptors: a brief overview. Clinical and Experimental Pharmacology and Physiology 26, 937–940. https://doi.org/10.1046/j.1440-1681.1999.03151.x

Chen, J.T., Guo, D., Campanelli, D., Frattini, F., Mayer, F., Zhou, L., Kuner, R., Heppenstall, P.A., Knipper, M., Hu, J., 2014. Presynaptic GABAergic inhibition regulated by BDNF contributes to neuropathic pain induction. Nature Communications 5, 5331.

Chen, Y., Willcockson, H.H., Valtschanoff, J.G., 2009. Vanilloid receptor TRPV1-mediated phosphorylation of ERK in murine adjuvant arthritis. Osteoarthritis and Cartilage 17, 244–251. https://doi.org/10.1016/j.joca.2008.06.015

Cho, W.G., Valtschanoff, J.G., 2008. Vanilloid receptor TRPV1-positive sensory afferents in the mouse ankle and knee joints. Brain Research 1219, 59–65. https://doi.org/10.1016/j.brainres.2008.04.043

da Silva Serra, I., Husson, Z., Bartlett, J.D., Smith, E.S., 2016. Characterization of cutaneous and articular sensory neurons. LID - 10.1177/1744806916636387 [doi] LID - 1744806916636387 [pii].

Davis, J.B., Gray, J., Gunthorpe, M.J., Hatcher, J.P., Davey, P.T., Overend, P., Harries, M.H., Latcham, J., Clapham, C., Atkinson, K., Hughes, S.A., Rance, K., Grau, E., Harper, A.J., Pugh, P.L., Rogers, D.C.,

Bingham, S., Randall, A., Sheardown, S.A., 2000. Vanilloid receptor-1 is essential for inflammatory thermal hyperalgesia. Nature 405, 183.

Deacon, R.M.J., 2006. Digging and marble burying in mice: simple methods for in vivo identification of biological impacts. Nature Protocols 1, 122.

Dittert, I., Benedikt, J., Vyklický, L., Zimmermann, K., Reeh, P.W., Vlachová, V., 2006. Improved superfusion technique for rapid cooling or heating of cultured cells under patch-clamp conditions. Journal of Neuroscience Methods 151, 178–185. https://doi.org/10.1016/j.jneumeth.2005.07.005

Djouhri, L., Bleazard, L., Lawson, S.N., 1998. Association of somatic action potential shape with sensory receptive properties in guinea-pig dorsal root ganglion neurones. The Journal of Physiology 513, 857–872. https://doi.org/10.1111/j.1469-7793.1998.857ba.x

Djouhri, L., Dawbarn, D., Robertson, A., Newton, R., Lawson, S.N., 2001. Time Course and Nerve Growth Factor Dependence of Inflammation-Induced Alterations in Electrophysiological Membrane Properties in Nociceptive Primary Afferent Neurons. J. Neurosci. 21, 8722.

Djouhri, L., Lawson, S.N., 1999. Changes in somatic action potential shape in guinea-pig nociceptive primary afferent neurones during inflammation in vivo. The Journal of Physiology 520, 565–576. https://doi.org/10.1111/j.1469-7793.1999.t01-1-00565.x

Farr, M., Garvey, K., Bold, A.M., Kendall, M.J., Bacon, P.A., 1985. Significance of the hydrogen ion concentration in synovial fluid in rheumatoid arthritis. Clin Exp Rheumatol 3, 99–104.

Fernandes, E.S., Russell, F.A., Alawi, K.M., Sand, C., Liang, L., Salamon, R., Bodkin, J.V., Aubdool, A.A., Arno, M., Gentry, C., Smillie, S.-J., Bevan, S., Keeble, J.E., Malcangio, M., Brain, S.D., 2016. Environmental cold exposure increases blood flow and affects pain sensitivity in the knee joints of CFA-induced arthritic mice in a TRPA1-dependent manner. Arthritis Research & Therapy 18, 7. https://doi.org/10.1186/s13075-015-0905-x

Fernandes, E.S., Russell, F.A., Spina, D., McDougall, J.J., Graepel, R., Gentry, C., Staniland, A.A., Mountford, D.M., Keeble, J.E., Malcangio, M., Bevan, S., Brain, S.D., 2011. A Distinct Role for Transient Receptor Potential Ankyrin 1, in Addition to Transient Receptor Potential Vanilloid 1, in Tumor Necrosis Factor alpha-Induced Inflammatory Hyperalgesia and Freund's Complete Adjuvant-Induced Monarthritis. Arthritis and Rheumatism 63, 819–829. https://doi.org/10.1002/art.30150

Fernandes, E.S., S, A., R, K., Brain, S., 2013. TRP Receptors in Arthritis, Gaining Knowledge for Translation from Experimental Models.

Flake, N.M., Gold, M.S., 2005. Inflammation alters sodium currents and excitability of temporomandibular joint afferents. Neuroscience Letters 384, 294–299. https://doi.org/10.1016/j.neulet.2005.04.091

Fujii, W., Kawahito, Y., Nagahara, H., Kukida, Y., Seno, T., Yamamoto, A., Kohno, M., Oda, R., Taniguchi, D., Fujiwara, H., Ejima, A., Kishida, T., Mazda, O., Ashihara, E., 2015. Monocarboxylate Transporter 4, Associated With the Acidification of Synovial Fluid, Is a Novel Therapeutic Target for Inflammatory Arthritis. Arthritis & Rheumatology 67, 2888–2896. https://doi.org/10.1002/art.39270

Garrison, S.R., Stucky, C.L., 2014. Contribution of Transient Receptor Potential Ankyrin 1 to Chronic Pain in Aged Mice With Complete Freund's Adjuvant–Induced Arthritis. Arthritis & Rheumatology 66, 2380–2390. https://doi.org/10.1002/art.38724

Gauldie, S.D., McQueen, D.S., Clarke, C.J., Chessell, I.P., 2004. A robust model of adjuvant-induced chronic unilateral arthritis in two mouse strains. J Neurosci Methods 139, 281–291. https://doi.org/10.1016/j.jneumeth.2004.05.003

Gregory, N., Harris, A., Robinson, C., Dougherty, P., Fuchs, P., Sluka, K., 2013. An overview of animal models of pain: disease models and outcome measures. The journal of pain : official journal of

751 the American Pain Society 14, 10.1016/j.jpain.2013.06.008.
752 https://doi.org/10.1016/j.jpain.2013.06.008
753 Grubb, B.D., Birrell, G.J., McQueen, D.S., Iggo, A., 1991. The role of PGE2 in the sensitization of
754 mechanoreceptors in normal and inflamed ankle joints of the rat. Experimental Brain Research
755 84, 383–392. https://doi.org/10.1007/BF00231460
756 Hannan, M.T., 1996. Epidemiologic perspectives on women and arthritis: An overview. Arthritis &
757 Rheumatism 9, 424–434. https://doi.org/10.1002/art.1790090603
758 Hawker, G.A., Stewart, L., French, M.R., Cibere, J., Jordan, J.M., March, L., Suarez-Almazor, M.,
759 Gooberman-Hill, R., 2008. Understanding the pain experience in hip and knee osteoarthritis – an
760 OARSI/OMERACT initiative. Osteoarthritis and Cartilage 16, 415–422.
761 https://doi.org/10.1016/j.joca.2007.12.017
762 Haywood, A.R., Hathway, G.J., Chapman, V., 2018. Differential contributions of peripheral and central
763 mechanisms to pain in a rodent model of osteoarthritis. Scientific Reports 8, 7122.
764 https://doi.org/10.1038/s41598-018-25581-8
765 Hillery, C.A., Kerstein, P.C., Vilceanu, D., Barabas, M.E., Retherford, D., Brandow, A.M., Wandersee, N.J.,
766 Stucky, C.L., 2011. Transient receptor potential vanilloid 1 mediates pain in mice with severe
767 sickle cell disease. Blood 118, 3376–3383. https://doi.org/10.1182/blood-2010-12-327429
768 Hockley, J.R.F., Taylor, T.S., Callejo, G., Wilbrey, A.L., Gutteridge, A., Bach, K., Winchester, W.J., Bulmer,
769 D.C., McMurray, G., Smith, E.S.J., 2018. Single-cell RNAseq reveals seven classes of colonic
770 sensory neuron. Gut. https://doi.org/10.1136/gutjnl-2017-315631
771 Holzer, P., 2009. Acid-sensitive ion channels and receptors. Handbook of experimental pharmacology
772 283–332. https://doi.org/10.1007/978-3-540-79090-7_9
773 Honore, P., Wismer, C.T., Mikusa, J., Zhu, C.Z., Zhong, C., Gauvin, D.M., Gomtsyan, A., El Kouhen, R., Lee,
774 C.-H., Marsh, K., Sullivan, J.P., Faltynek, C.R., Jarvis, M.F., 2005. A-425619 [1-Isoquinolin-5-yl-3-
775 (4-trifluoromethyl-benzyl)-urea], a Novel Transient Receptor Potential Type V1 Receptor
776 Antagonist, Relieves Pathophysiological Pain Associated with Inflammation and Tissue Injury in
777 Rats. J Pharmacol Exp Ther 314, 410. https://doi.org/10.1124/jpet.105.083915
778 Hsieh, W.-S., Kung, C.-C., Huang, S.-L., Lin, S.-C., Sun, W.-H., 2017. TDAG8, TRPV1, and ASIC3 involved in
779 establishing hyperalgesic priming in experimental rheumatoid arthritis. Scientific Reports 7,
780 8870. https://doi.org/10.1038/s41598-017-09200-6
781 Ikeuchi, M., Kolker, S.J., Sluka, K.A., 2009. Acid-sensing ion channel 3 expression in mouse knee joint
782 afferents and effects of carrageenan-induced arthritis. J Pain 10.
783 https://doi.org/10.1016/j.jpain.2008.10.010
784 Ji, R.-R., Samad, T.A., Jin, S.-X., Schmoll, R., Woolf, C.J., 2002. p38 MAPK Activation by NGF in Primary
785 Sensory Neurons after Inflammation Increases TRPV1 Levels and Maintains Heat Hyperalgesia.
786 Neuron 36, 57–68. https://doi.org/10.1016/S0896-6273(02)00908-X
787 Jirkof, P., 2014. Burrowing and nest building behavior as indicators of well-being in mice. Journal of
788 Neuroscience Methods 234, 139–146. https://doi.org/10.1016/j.jneumeth.2014.02.001
789 Keeble, J., Russell, F., Curtis, B., Starr, A., Pinter, E., Brain, S.D., 2005. Involvement of transient receptor
790 potential vanilloid 1 in the vascular and hyperalgesic components of joint inflammation. Arthritis
791 and Rheumatism 52, 3248–3256. https://doi.org/10.1002/art.21297
792 Kim, Y.., Na, H.., Kim, S.., Han, H.., Yoon, Y.., Sung, B., Nam, H.., Shin, S.., Hong, S.., 1998. Cell type-
793 specific changes of the membrane properties of peripherally-axotomized dorsal root ganglion
794 neurons in a rat model of neuropathic pain. Neuroscience 86, 301–309.
795 https://doi.org/10.1016/S0306-4522(98)00022-0
796 Lawson, S.N., McCarthy, P.W., Prabhakar, E., 1996. Electrophysiological properties of neurones with
797 CGRP-like immunoreactivity in rat dorsal root ganglia. Journal of Comparative Neurology 365,
798 355–366. https://doi.org/10.1002/(SICI)1096-9861(19960212)365:3<355::AID-CNE2>3.0.CO;2-3

799 Lee, K.Y., Charbonnet, M., Gold, M.S., 2012. Upregulation of high affinity GABA(A) receptors in cultured
800 rat dorsal root ganglion neurons. Neuroscience 208C, 133–142.
801 https://doi.org/10.1016/j.neuroscience.2012.01.050
802 Lewis, T., 1938. Study of Somatic Pain. British Medical Journal 1, 321–325.
803 Li, C.-L., Li, K.-C., Wu, D., Chen, Y., Luo, H., Zhao, J.-R., Wang, S.-S., Sun, M.-M., Lu, Y.-J., Zhong, Y.-Q., Hu,
804 X.-Y., Hou, R., Zhou, B.-B., Bao, L., Xiao, H.-S., Zhang, X., 2015. Somatosensory neuron types
805 identified by high-coverage single-cell RNA-sequencing and functional heterogeneity. Cell
806 Research 26, 83.
807 Meziane, H., Ouagazzal, A. -M., Aubert, L., Wietrzych, M., Krezel, W., 2007. Estrous cycle effects on
808 behavior of C57BL/6J and BALB/cByJ female mice: implications for phenotyping strategies.
809 Genes, Brain and Behavior 6, 192–200. https://doi.org/10.1111/j.1601-183X.2006.00249.x
810 Moilanen, L.J., Laavola, M., Kukkonen, M., Korhonen, R., Leppänen, T., Högestätt, E.D., Zygmunt, P.M.,
811 Nieminen, R.M., Moilanen, E., 2012. TRPA1 Contributes to the Acute Inflammatory Response
812 and Mediates Carrageenan-Induced Paw Edema in the Mouse. Scientific Reports 2, 380.
813 Moore, C., Gupta, R., Jordt, S.-E., Chen, Y., Liedtke, W.B., 2018. Regulation of Pain and Itch by TRP
814 Channels. Neuroscience Bulletin 34, 120–142. https://doi.org/10.1007/s12264-017-0200-8
815 Petrus, M., Peier, A.M., Bandell, M., Hwang, S.W., Huynh, T., Olney, N., Jegla, T., Patapoutian, A., 2007. A
816 role of TRPA1 in mechanical hyperalgesia is revealed by pharmacological inhibition. Molecular
817 Pain 3, 40–40. https://doi.org/10.1186/1744-8069-3-40
818 Price, M.P., McIlwrath, S.L., Xie, J., Cheng, C., Qiao, J., Tarr, D.E., Sluka, K.A., Brennan, T.J., Lewin, G.R.,
819 Welsh, M.J., 2001. The DRASIC Cation Channel contributes to the detection of cutaneous touch
820 and acid stimuli in mice. Neuron 32. https://doi.org/10.1016/S0896-6273(01)00547-5
821 Rice, A.S.C., Cimino-Brown, D., Eisenach, J.C., Kontinen, V.K., Lacroix-Fralish, M.L., Machin, I., Mogil, J.S.,
822 Stöhr, T., 2008. Animal models and the prediction of efficacy in clinical trials of analgesic drugs:
823 A critical appraisal and call for uniform reporting standards. PAIN 139, 243–247.
824 https://doi.org/10.1016/j.pain.2008.08.017
825 Rigaud, M., Gemes, G., Barabas, M.-E., Chernoff, D.I., Abram, S.E., Stucky, C.L., Hogan, Q.H., 2008.
826 Species and strain differences in rodent sciatic nerve anatomy: Implications for studies of
827 neuropathic pain. Pain 136, 188–201. https://doi.org/10.1016/j.pain.2008.01.016
828 Rutten, K., Robens, A., Read, S.J., Christoph, T., 2014. Pharmacological validation of a refined burrowing
829 paradigm for prediction of analgesic efficacy in a rat model of sub-chronic knee joint
830 inflammation. European Journal of Pain 18, 213–222. https://doi.org/10.1002/j.1532-
831 2149.2013.00359.x
832 Samer R Eid, Eric D Crown, Eric L Moore, Hongyu A Liang, Kar-Chan Choong, Shelley Dima, Darrell A
833 Henze, Stefanie A Kane, Mark O Urban, 2008. HC-030031, a TRPA1 Selective Antagonist,
834 Attenuates Inflammatory- and Neuropathy-Induced Mechanical Hypersensitivity. Mol Pain 4,
835 1744-8069-4–48. https://doi.org/10.1186/1744-8069-4-48
836 Sara Nencini, Mitchell Ringuet, Dong-Hyun Kim, Yu-Jen Chen, Claire Greenhill, Jason J Ivanusic, 2017.
837 Mechanisms of nerve growth factor signaling in bone nociceptors and in an animal model of
838 inflammatory bone pain. Mol Pain 13, 1744806917697011.
839 https://doi.org/10.1177/1744806917697011
840 Schaible, H.-G., Ebersberger, A., von Banchet, G.S., 2002. Mechanisms of Pain in Arthritis. Annals of the
841 New York Academy of Sciences 966, 343–354. https://doi.org/10.1111/j.1749-
842 6632.2002.tb04234.x
843 Scott, B.S., Edwards, B.A., 1980. Electric membrane properties of adult mouse DRG neurons and the
844 effect of culture duration. J Neurobiol 11, 291–301. https://doi.org/10.1002/neu.480110307
845 Seidel, M.F., Wise, B.L., Lane, N.E., 2013. Nerve growth factor: an update on the science and therapy.
846 Osteoarthritis and Cartilage 21, 1223–1228. https://doi.org/10.1016/j.joca.2013.06.004

847 Shepherd, A.J., Cloud, M.E., Cao, Y.-Q., Mohapatra, D.P., 2018. Deficits in Burrowing Behaviors Are
848 Associated With Mouse Models of Neuropathic but Not Inflammatory Pain or Migraine.
849 Frontiers in Behavioral Neuroscience 12, 124. https://doi.org/10.3389/fnbeh.2018.00124
850 Sluka, K.A., Price, M.P., Breese, N.M., Stucky, C.L., Wemmie, J.A., Welsh, M.J., 2003. Chronic hyperalgesia
851 induced by repeated acid injections in muscle is abolished by the loss of ASIC3, but not ASIC1.
852 Pain 106. https://doi.org/10.1016/S0304-3959(03)00269-0
853 Smith, E.S.J., Omerbašić, D., Lechner, S.G., Anirudhan, G., Lapatsina, L., Lewin, G.R., 2011. The Molecular
854 Basis of Acid Insensitivity in the African Naked Mole-Rat. Science 334, 1557.
855 https://doi.org/10.1126/science.1213760
856 St. John Smith, E., 2018. Advances in understanding nociception and neuropathic pain. Journal of
857 Neurology 265, 231–238. https://doi.org/10.1007/s00415-017-8641-6
858 Staniland, A.A., McMahon, S.B., 2009. Mice lacking acid-sensing ion channels (ASIC) 1 or 2, but not
859 ASIC3, show increased pain behaviour in the formalin test. European Journal of Pain 13, 554–
860 563. https://doi.org/10.1016/j.ejpain.2008.07.001
861 Story, G.M., Peier, A.M., Reeve, A.J., Eid, S.R., Mosbacher, J., Hricik, T.R., Earley, T.J., Hergarden, A.C.,
862 Andersson, D.A., Hwang, S.W., McIntyre, P., Jegla, T., Bevan, S., Patapoutian, A., 2003. ANKTM1,
863 a TRP-like Channel Expressed in Nociceptive Neurons, Is Activated by Cold Temperatures. Cell
864 112, 819–829. https://doi.org/10.1016/S0092-8674(03)00158-2
865 Sung, K.-W., Kirby, M., McDonald, M.P., Lovinger, D.M., Delpire, E., 2000. Abnormal $GABA_A$ Receptor-
866 Mediated Currents in Dorsal Root Ganglion Neurons Isolated from Na–K–2Cl Cotransporter Null
867 Mice. J. Neurosci. 20, 7531.
868 Sutherland, F.I., Bannatyne, B.A., Kerr, R., Riddell, J.S., Maxwell, D.J., 2002. Inhibitory amino acid
869 transmitters associated with axons in presynaptic apposition to cutaneous primary afferent
870 axons in the cat spinal cord. J Comp Neurol 452, 154–162. https://doi.org/10.1002/cne.10374
871 Treharne, G.J., Kitas, G.D., Lyons, A.C., Booth, D.A., 2005. Well-being in Rheumatoid Arthritis: The Effects
872 of Disease Duration and Psychosocial Factors. J Health Psychol 10, 457–474.
873 https://doi.org/10.1177/1359105305051416
874 Usoskin, D., Furlan, A., Islam, S., Abdo, H., Lonnerberg, P., Lou, D., Hjerling-Leffler, J., Haeggstrom, J.,
875 Kharchenko, O., Kharchenko, P.V., Linnarsson, S., Ernfors, P., 2015. Unbiased classification of
876 sensory neuron types by large-scale single-cell RNA sequencing. Nat Neurosci 18, 145–153.
877 Vilen, L., Baldassari, A.R., Callahan, L.F., 2017. Socioeconomic burden of pain in rheumatic disease. Clin
878 Exp Rheumatol 35 Suppl 107, 26–31.
879 Weng, X., Smith, T., Sathish, J., Djouhri, L., 2012. Chronic inflammatory pain is associated with increased
880 excitability and hyperpolarization-activated current (Ih) in C- but not Aδ-nociceptors. PAIN® 153,
881 900–914. https://doi.org/10.1016/j.pain.2012.01.019
882 Willis, W.D.J., 1999. Dorsal root potentials and dorsal root reflexes: a double-edged sword. Exp Brain Res
883 124, 395–421.
884 Winter, J., Alistair Forbes, C., Sternberg, J., Lindsay, R.M., 1988. Nerve growth factor (NGF) regulates
885 adult rat cultured dorsal root ganglion neuron responses to the excitotoxin capsaicin. Neuron 1,
886 973–981. https://doi.org/10.1016/0896-6273(88)90154-7
887 Wright, A.J., Husson, Z.M.A., Hu, D.-E., Callejo, G., Brindle, K.M., Smith, E.S.J., 2018. Increased
888 hyperpolarized [1-13C] lactate production in a model of joint inflammation is not accompanied
889 by tissue acidosis as assessed using hyperpolarized 13C-labelled bicarbonate. NMR in
890 Biomedicine e3892–n/a. https://doi.org/10.1002/nbm.3892
891 Yu, L., Yang, F., Luo, H., Liu, F.Y., Han, J.S., Xing, G.G., Wan, Y., 2008. The role of TRPV1 in different
892 subtypes of dorsal root ganglion neurons in rat chronic inflammatory nociception induced by
893 complete Freund's adjuvant. Mol Pain 4. https://doi.org/10.1186/1744-8069-4-61

894 Zhang, R.-X., Ren, K., Dubner, R., 2013. Osteoarthritis pain mechanisms: Basic studies in animal models.
895 Osteoarthritis and cartilage / OARS, Osteoarthritis Research Society 21, 1308–1315.
896 https://doi.org/10.1016/j.joca.2013.06.013
897 Zhang, X., Huang, J., McNaughton, P.A., 2005. NGF rapidly increases membrane expression of TRPV1
898 heat-gated ion channels. EMBO J 24, 4211. https://doi.org/10.1038/sj.emboj.7600893
899 Zhang, X., Lee, K.-Y., Priest, B.T., Belfer, I., Gold, M.S., 2015. Inflammatory mediator-induced modulation
900 of GABA(A) currents in human sensory neurons. Neuroscience 310, 401–409.
901 https://doi.org/10.1016/j.neuroscience.2015.09.048
902 Zhou, Y., Li, G.-D., Zhao, Z.-Q., 2003. State-dependent phosphorylation of ε-isozyme of protein kinase C
903 in adult rat dorsal root ganglia after inflammation and nerve injury. Journal of Neurochemistry
904 85, 571–580. https://doi.org/10.1046/j.1471-4159.2003.01675.x
905 Zhu, Y., Lu, S., Gold, M.S., 2012. Persistent inflammation increases GABA-induced depolarization of rat
906 cutaneous dorsal root ganglion neurons in vitro. Neuroscience 220, 330–340.
907 https://doi.org/10.1016/j.neuroscience.2012.06.025
908

909

910 Supplementary Digital Content 1: Video that shows a mouse digging after FB injection in the knee

911 (left) and after CFA injection in the knee (right).mp4

912

Table 1: Properties of knee-innervating dorsal root ganglion neurons from the CFA injected side (CFA) and contralateral side (Cntrl) across time-in-culture. * = significance test of CFA vs Cntrl neurons in the same time group by unpaired t-test, # = significance test of CFA neurons amongst the three time points by ANOVA, ^ = significance test of Cntrl neurons amongst the three time points by ANOVA. */#/^ indicates $p < 0.05$, **/##/^^^ indicates $p < 0.01$, ***/###/^^^ indicates $p < 0.0001$.

	4-hour				24-hour				48-hour			
	CFA (n = 25)		Cntrl (n = 27)		CFA (n = 25)		Cntrl (n = 22)		CFA (n = 23)		Cntrl (n = 22)	
	Mean	SEM	Mean	SEM	Mean	SEM	Mean	SEM.	Mean	SEM	Mean	SEM
RMP (mV)	-55.7	2.1	-58.3	1.6	-55.3	1.3	-52.5	1.9	-55.6	1.3	-54.6	1.8
Diameter (mm)	31.5	0.7	31.9	0.5	31.6	0.8	32.6	0.9	29.2	0.8	29.1	1.1
Capacitance (pF)	45.7	4.2	58.2	4.2	53.8	5.6	52.9	8.2	36.2	4.6	48.5	6.4
Threshold (pA)	384.0	44.3	550.0*	48.3	473.6	42.9	682.7**	48.1	552.2	72.1	475.5	67.5
Half peak duration (HPD, ms)	1.3	0.2	1.0	0.1	1.0	0.2	1.7	0.3	2.1##	0.4	2.6^^^	0.4
Afterhypolarization (AHP, ms)	8.6**	1.0	4.9	0.8	10.8	2.0	7.9	1.5	10.9	1.9	14.3^^^	2.2
Afterhyperpolarization amplitude (AHP amplitude, mV)	16.1	0.8	13.8	0.9	16.5	0.9	14.2	0.9	14.1	1.0	16.8	1.4
Amplitude (mV)	88.2	4.8	86.2	4.6	79.3	5.1	68.3	6.4	82.7	4.6	83.1	5.5

Table 2: Sustained peak current densities of CFA and Cntrl DRG neurons in response to acid, TRP channel agonists (capsaisin, cinnamaldehyde and menthol) and GABA across time-in-culture. # = significance test of CFA neurons amongst the three time points by ANOVA, ^ = significance test of Cntrl neurons amongst the three time points by ANOVA. #/^ indicates $p < 0.05$, ##/^^^ indicates $p < 0.01$, ###/^^^ indicates $p < 0.0001$.

Treatment	4-hour						24-hour						48-hour					
	CFA			Cntrl			CFA			Cntrl			CFA			Cntrl		
	Mean	SEM	n	Mean	SEM.	n	Mean	SEM	n	Mean	SEM	n	Mean	SEM	n	Mean	SEM	n
pH 7	1.0	0.2	19	0.6	0.08	23	4.0##	1.0	19	5.7^^^	1.5	17	1.5	0.5	14	1.5	2.7	15
pH 6	2.6	0.9	21	1.5	0.3	25	4.0	0.7	20	5.3	1.6	19	5.8	1.4	22	4.9	1.9	19
pH 5	5.3	2.3	20	2.3	0.3	23	14.9	4.3	21	14.5^^	4.2	19	7.4	1.4	19	7.9	2.9	15
Capsaicin	4.4	2.8	18	0.8	0.1	12	1.8	0.5	22	4.6	2.1	11	10.3	5.1	13	6.4	4.0	10
Cinnamaldehyde	0.8	0.2	10	0.7	0.09	18	2.2	0.4	19	2.3	0.7	14	0.9	0.3	8	2.5	2.0	5
Menthol	0.8	0.2	9	0.9	0.2	14	1.0	0.2	12	1.6	0.4	9	1.2	0.7	8	2.8	2.2	3
GABA	7.2	2.0	19	3.9	1.1	26	11.8*	2.6	22	4.3	0.9	19	8.3	2.7	18	4.3	1.7	16

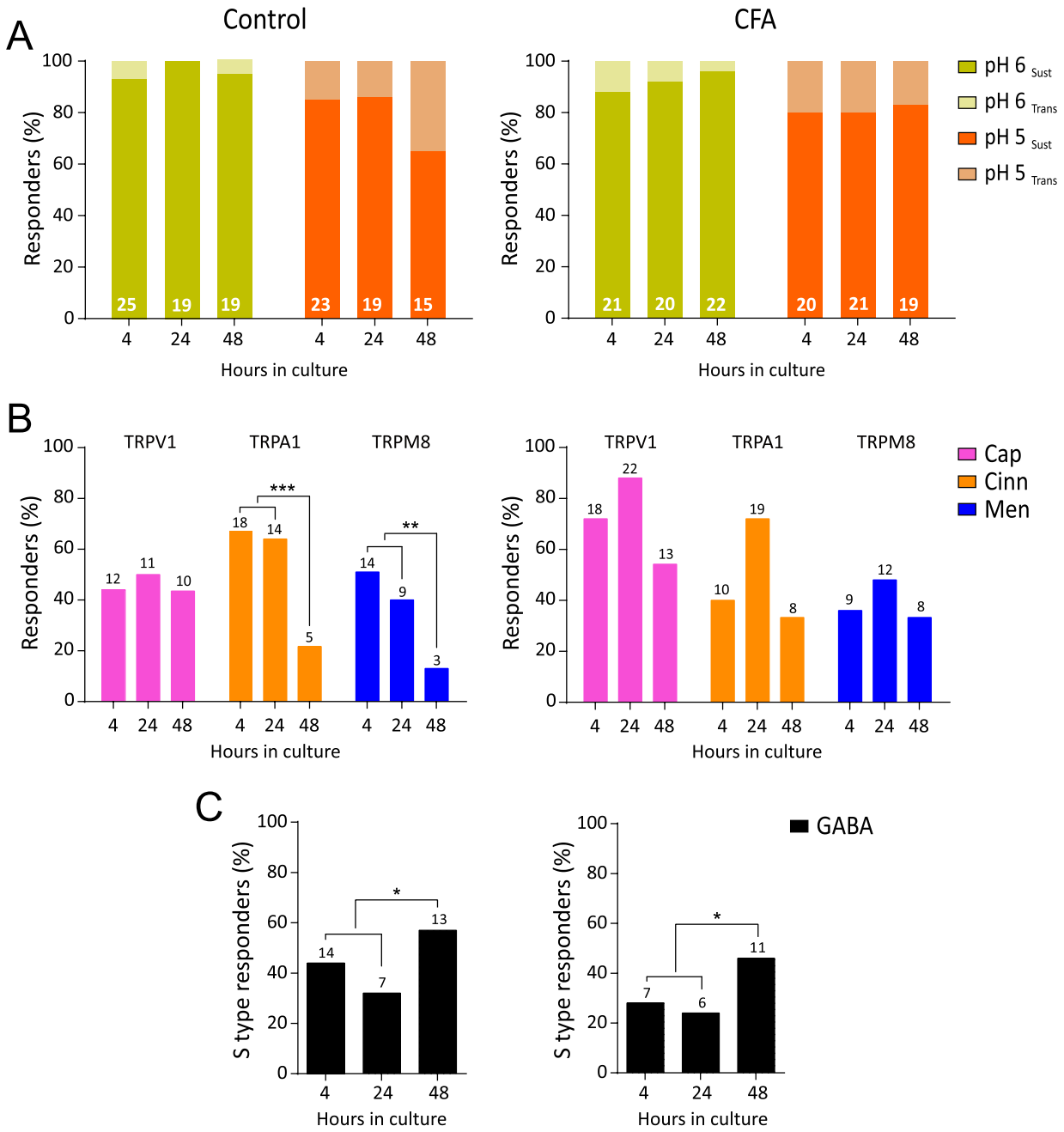

Supplementary Digital Content 2: Figure showing time-in-culture effects on acid, TRP agonist and GABA sensitivity of knee neurons after inflammation.pdf

A) Proportion of Cntrl (left) and CFA (right) neurons responding to pH 6 (yellow) and pH 5 (orange) with a transient + sustained type current (light shade) and sustained only type current (dark shade) across 4, 24 and 48-hours. B) Percentage frequency of Cntrl (left) and CFA (right) neurons sensitive to capsaicin (pink), cinnamaldehyde (orange) and menthol (blue) across 4, 24 and 48-hours in culture. C) Percentage of Cntrl (left) and CFA (right) neurons that had a sustained GABA-evoked current across 4, 24 and 48-hours in culture. * indicates $p < 0.05$, chi-sq test. The numbers above the bars indicate the number of responsive neurons.